Hygrothermal Effects on Viscoelastic Properties of Amine-Hardened Epoxy

by

Ernesto Leon

A thesis
presented to the University of Waterloo
in fulfillment of the
thesis requirement for the degree of
Master of Applied Science
in
Mechanical Engineering

Waterloo, Ontario, Canada, 2015

AUTHOR'S DECLARATION

I hereby declare that I am the sole author of this thesis. This is a true copy of the thesis, including any required final revisions, as accepted by my examiners.

I understand that my thesis may be made electronically available to the public.

Abstract

In this work the behaviour of a DGEBA/TETA epoxy resin system, a candidate resin for electrically conductive nanocomposites, has been characterized after exposure to hygrothermal conditions for up to 2400 hours. The objectives of the study were to determine the diffusion coefficient, the viscoelastic and glass transition temperature changes as result of long-term aging. Due to the large number of samples required, inherent material properties and physical constraints of the measurement instruments, significant efforts were made to develop an appropriate molding technique to fabricate consistently high quality samples. Over 200 thin samples were fabricated for gravimetric measurements and dynamic mechanical analysis (DMA) testing at iso-strain and temperature-sweep.

As far as we know, this is the first known comprehensive report of the variation of storage modulus as a function of time, temperature and water uptake for an epoxy resin system. When room temperature DMA tests were conducted on progressively aged samples, we found material behaviour to be highly dependent on the hygrothermal aging conditions, such as temperature, relative humidity and exposure time. In the case of storage modulus, it was found that higher dry aging temperature can be detrimental on the modulus as exposure time increased. This effect, however, was attenuated when coupled with relative humidity conditions where the modulus values increased. This behaviour can be associated with reported hydrogen bonding mechanisms occurring in the material.

When tests were conducted after at least 80 days of aging using temperature ramp-up in the DMA, the reverse is found. The effects of structural relaxation of physical aging including volumetric contraction became evident during ramp-up. For dry aging condition samples, the storage modulus increased while relative humidity conditions reduced it, consistent with plasticization. It would appear then that the temperature ramp-up method is able to delineate physical aging and plasticization effects prior to the onset of glass transition.

Finally, the glass transition temperature is greatly influenced by hygrothermal conditions. The results for the different conditions in this study can be interpreted using various theoretical concepts published in the open literature. They include the formation of hydrogen bonds between the water molecules and the OH groups of the epoxy. Loss modulus and *tan* δ as measured by DMA indicated that the former tends to be more sensitive than the latter, better discerning the effects of relative humidity.

Keywords: DGEBA/TETA, diffusion, relative humidity, glass transition temperature, storage modulus.

Acknowledgements

I am deeply indebted to my supervisor Dr. Pearl Sullivan for her guidance and encouragement in this research work; I am very grateful I was given this opportunity at a time polymer science was a novel area for me.

Funding for this research was provided by Blackberry Ltd and the Natural Science and Engineering Research Council of Canada (NSERC): their contributions are gratefully acknowledged. Special thanks to Dr. Sina Chaechian for his invaluable assistance during the development of the experimental setup and to my colleagues working at the Advanced Polymers and Composites group at the University of Waterloo: Geoff Rivers and Allan Rogalsky for their company and insightful discussions about research.

I would also like to mention the invaluable cooperation of Dr. Dwayne Wasylyshyn and personnel working at the Materials Laboratory at Blackberry Ltd for permitting the use of the necessary equipment for the experimentation.

Special thanks to my parents, sisters and loved ones who have contributed to my formation, always listening and very supportive.

Dedication

I dedicate this work to my parents, sisters and loved ones: without their love and support I would not be here in the first place.

Table of Contents

List of Figures

List of Tables

Nomenclature

∇	Gradient
$\nabla \cdot$	Divergence
A	Cross sectional area
ANOVA	Analysis of Variance
ASTM	American Society for Testing and Materials
C	Moisture concentration
C_∞	Equilibrium moisture concentration
C_i	Initial moisture concentration
D	Diffusion coefficient or Diffusivity
D_c	Corrected diffusion coefficient
DDA	Dicyandiamide
DDS	Diaminodiphenylsulfone
DETA	Diethylenetriamine
DETDA	Diethyltoluene diamine
DGEBA	Diglycidyl Ether of Bisphenol A
DMA	Dynamic Mechanical Analysis
DSC	Differential Scanning Calorimetry
DTA	Diethyltoluene diamine
E	Modulus of elasticity
E'	Storage modulus
E"	Loss modulus
E*	Complex modulus
h	Thickness

IC	Integrated circuit
IEC	International Electrotechnical Commission
Ks	Measured stiffness
l	Length
M_d	Mass of the dry sample
M_s or M_∞	Moisture uptake at equilibrium
M_t	Moisture uptake at time t
mDPA	Metaphenylene diamine
PDMS	Polydimethylsiloxane
phr	Parts per hundred
PTFE	Polytetrafluoroethylene (Teflon)
RH	Relative humidity, %
SD	Standard deviation
t	Time
T	Temperature
TETA	Triethylenetetramine
T_f	Film temperature
T_g	Glass transition temperature
$T_{g\infty}$	Ultimate glass transition temperature
$T_{g,wet}$	Wet glass transition temperature
TGDDM	tetraglycidyl-4,4-diaminodiphenyl methane
w	Width
x	x-coordinate
y	y-coordinate

z	z-coordinate
δ	Phase angle
ρ	Density

Chapter 1
Introduction

1.1 Hygrothermal Aging in Epoxy Resins

Epoxy resins are thermosetting polymers that are widely used for coating, molding and encapsulation because of their excellent mechanical properties after curing. Typical applications are in microelectronic devices, medical implants, and aircraft structures. Certain combined conditions of heat and high humidity, or hygrothermal conditions, can be detrimental to their application, especially if mechanical integrity is affected. Epoxies are used in stand-alone "neat" resins and as matrix resins for composites in many applications; however, they are hygroscopic due to the presence of polar groups that attract water, generating reversible and irreversible phenomena, such as plasticization, hydrolysis and crazing when the hygrothermal exposures reach specific conditions.

1.2 Motivation and Scope of Work

One of the fundamental challenges of the application of engineering materials in industry is the prediction of lifetime service when these materials are exposed to environmental conditions. As reported in the literature [1-3], combined long-term exposure to heat and moisture can reduce the mechanical properties of polymers. Thermosetting polymers, such as diglycidyl ether of bisphenol-A hardened with triethylenetetramine (DGEBA/TETA), even though relatively strong because of their tri-dimensional network crosslinking, can be affected when used either as a neat resin or as a matrix for composites when exposed to harsh hygrothermal conditions. One of the practical applications of epoxy is as a component in integrated circuit (IC) device packages [4]. When epoxies are combined with fillers and other material, certain interactions can occur in different environmental conditions; thus, it is important that the base resin be evaluated for a long period, in both ambient and service conditions. The most common approach to long-term testing is with the use of temperature-humidity chambers to test the reliability of an electronic device subjected to constant and cyclic temperature and humidity conditions. Standards, such as IEC 60068-2-38 and IEC 60068-2-78, used in the electronics industry cite common temperature-humidity severity ranging from 30 °C to 40 °C in temperature and up to 93% in Relative Humidity (RH). Research on the action of various relative humidity and temperature combinations to DGEBA/TETA epoxies has been a minor focus in the literature; instead most studies have considered only the immersed

condition. Since most service conditions are not immersive, the present thesis aims to conduct studies to characterize the effects of various temperatures and relative humidity combinations on the thermo-mechanical properties of a DGEBA/TETA epoxy.

1.3 Objectives of Work

The main objective of this research work is to study the effects of thermal and hygrothermal aging of an amine-hardened epoxy being considered as a candidate resin for the development of electrically conductive nanocomposite. To fulfill this objective, the scope of work has included the following:

1. To study the effect of thermal aging and hygrothermal aging on the elastic modulus and damping properties, as respectively measured by the storage modulus and loss modulus using a Dynamic Mechanical Analyzer (DMA).
2. To correlate the DMA study with glass transition temperature, moisture uptake behaviour and diffusion parameters in the epoxy material.

1.4 Anticipated Contributions to the Field

Research on the storage modulus and loss modulus of amine-hardened epoxy resins undergoing isothermal aging and hygrothermal aging has been very limited, especially for exposures to various RH environments. Much of the reported work has focused on the effects on the glass transition temperature (T_g) instead, since the value of the glass transition influences the epoxy service temperature [2, 5]. However, studies on storage and loss moduli in epoxies have reported conflicting results, including increases as well as decreases, while others have noted no change in behaviour [6, 7]. Some observed that the storage modulus is neither affected by the cross-link density nor the moisture uptake in the glassy state. Still others, however, have found variations of about 30% in reduction during the rapidly absorbing phase of water diffusion [8-11]. Finally, some researchers have found slightly shaped bell curves peaking at about the mid-point of the rapidly absorbing phase of moisture penetration [12].

The moisture uptake curves derived from the gravimetric analysis, and the subsequent determination of the type of diffusion model (i.e. Fickian or non-Fickian) is a common technique applied to study polymer material behaviour when exposed to relative humidity conditions.

This study is intended to determine the behaviour of a DGEBA/TETA amine-hardened epoxy when subjected to a set of hygrothermal conditions.

1.5 Presentation of Thesis

This thesis contains five chapters, presented as follows: Chapter 1 has introduced the problem statement, objectives and the contributions of this research. Chapter 2 addresses the theoretical background and past research work, fundamental to understanding and solving the problem. Chapter 3 presents the methodology, techniques and instruments used through the project. Chapter 4 details the results and relevant observations; and finally, Chapter 5 draws conclusions and suggests future work in the area.

Chapter 2
Background and Literature Review

This section provides: (i) the theoretical formulations to describe diffusion; (ii) a description of dynamic mechanical properties including storage modulus, loss modulus, glass transition temperature, and (iii) a background overview of the effects that moisture and aging have on them. In addition, the results of a comprehensive literature review of the research area have also been included.

2.1 Diffusion

In order to describe the movement of moisture within epoxies, the concepts of diffusion and difference between Fickian and Non-Fickian diffusion are provided here.

Diffusion is the phenomenon in which a substance moves from a region of high concentration gradient to another of low concentration gradient. For a process involving moisture absorption into a polymeric material, the most common approach is to use Fick's law of diffusion, which considers the rate of diffusion to be constant and describes the behaviour of water uptake in the form of [4, 13]:

$$\frac{\partial C}{\partial t} = \nabla \cdot (D\, \nabla C) \tag{2.1}$$

For an isotropic material:

$$\frac{\partial C}{\partial t} = D\left(\frac{\partial^2 C}{\partial x^2} + \frac{\partial^2 C}{\partial y^2} + \frac{\partial^2 C}{\partial z^2}\right) \tag{2.2}$$

where C (g/mm^3) is the moisture concentration, t (s) is time, D is the diffusion coefficient (mm^2/s), and x, y and z (mm) are the axes along the concentration gradient.

This equation results, from the premise that the temperature and the diffusivity inside the material are constant. If the moisture through the edges is neglected (i.e. thin plate: $h/l << 1$ and $h/w << 1$), and appropriate boundary conditions are considered, then the one-dimensional case is [13]:

$$\frac{\partial C}{\partial t} = D\frac{\partial^2 C}{\partial x^2} \tag{2.3}$$

$$C = C_i \qquad 0 < x < h \qquad t \leq 0$$
$$C = C_\infty \qquad x = 0,\ x = h \qquad t > 0$$

where C_i is the initial concentration and C_∞ is the maximum equilibrium moisture concentration. The solution of the equation above, given the boundary conditions is [13]:

$$\frac{C(t,x) - C_i}{C_\infty - C_i} = 1 - \frac{4}{\pi^2}\sum_{j=0}^{\infty}\frac{1}{(2j+1)^2}\sin\frac{(2j+1)\,\pi\,x}{h}\exp\left(-\frac{(2j+1)^2\pi^2 D}{h^2}t\right) \tag{2.4}$$

The amount of moisture C_i initially present in the material is generally zero, so $C(t, x)$ and C_∞ are effectively M_t and M_∞ respectively. M_t is moisture uptake at time t and the equilibrium moisture gain in the specimen at saturation is M_∞.

$$C(t,x) - C_i = M_t \tag{2.5}$$

$$C_\infty - C_i = M_\infty \tag{2.6}$$

An analytical solution of the moisture weight gain is obtained from integrating the concentration over plate thickness h [4]:

$$\frac{M_t}{M_\infty} = 1 - \frac{8}{\pi^2}\sum_{j=0}^{\infty}\frac{1}{(2j+1)^2}\exp\left(-\frac{(2j+1)^2\pi^2 D}{h^2}t\right) \tag{2.7}$$

An approximate solution to the above equation is [13]:

$$\frac{M_t}{M_\infty} = 1 - exp\left(-7.3\left(\frac{D\,t}{h^2}\right)^{0.75}\right) \tag{2.8}$$

and solved for D is:

$$D = \frac{h^2}{t}\left(-\frac{\ln\left(1 - \frac{M_t}{M_\infty}\right)}{7.3}\right)^{4/3} \tag{2.9}$$

Alternatively, during the initial linear part of the diffusion process ($M_t/M_\infty < 0.6$) D can be obtained by the following expression:

$$\frac{M_t}{M_\infty} = 4\left(\frac{D\,t}{\pi\,h^2}\right)^{1/2} \tag{2.10}$$

And when solving for D:

$$D = \frac{\pi}{16\,t}\left(h\,\frac{M_t}{M_\infty}\right)^2 \tag{2.11}$$

Since the diffusivity equation is idealized for one-dimensional case (i.e. very thin specimen), it is necessary to consider the effect of diffusion through the edges of the sample with equation 2.12 [13]. In this equation *h*, *l*, and *w* are the thickness, length and width of the samples respectively.

$$D_c = D\left(1 + \frac{h}{l} + \frac{h}{w}\right)^{-2} \tag{2.12}$$

For the moisture uptake analysis, the following equation shows the mass uptake:

$$Moisture\ Uptake\ (\%) = \frac{M_t - M_d}{M_d}\ x\ 100 \tag{2.13}$$

where M_t is the weight of the sample at time *t*, and M_d is the initial weight (before conditioning).

Since Fick's model considers that the sorbed resides in the free volume and that no interaction is present (i.e. relaxation or degradation effects on the polymer are not considered), it may not be completely accurate as a predictive tool, especially since some authors have observed strong bonding between water and epoxy groups at later stages in the absorption process. However, for the purpose of determining the diffusion coefficient of the epoxy it seems to yield acceptable results [14], thus the Fickian model will be the one used to calculate this parameter.

2.2 Effects of moisture absorption on thermomechanical properties

The glass transition temperature is the temperature boundary at which the polymer observes a strong change in its free volume and relaxation times [15]. When the temperature is above the polymer's T_g, the energy necessary for the cooperative movement of the local segments towards equilibrium is exceeded

allowing the molecules to slide past each other; this state is called "rubbery state" due to the softening of the material. As the polymer cools down below its T_g, the small molecular motions are arrested, limiting the mobility and increasing the stiffness of the material in a state known as the "glassy state". The temperature at which this phenomenon occurs is, thus, a key factor in the selection of polymers towards different applications.

Among the studies on the physico-mechanical property changes in polymers due to water sorption, the literature reports three principal mechanisms at play: plasticization, hydrolysis and crazing. When water molecules are in direct contact with the polymer system, configurational changes of the polymer chains together with random walk are part of the process that fills the free microvolumes [16]. During this process, Type I hydrogen-bonding starts forming and causing hygroscopic swelling and a phenomenon known as plasticization which debilitates the structure by increasing the relative movement of the molecules in the cross-linked network. This generates an increase in internal stresses [17] and a reduction of the glass transition temperature, which is then referred to as "wet" glass transition temperature $T_{g,wet}$, creating an additional detrimental effect in the form of reduced yield stress. In most cases, the water uptake is more influential in reducing the stiffness of the material when the surrounding temperature is between 50 °C below the $T_{g,wet}$ and the dry T_g [2].

If the polymer is kept in the presence of water for a longer time, stronger hydrogen bonding, Type II between water molecules and epoxy starts occurring. These hydrogen bondings are classified into Type I and Type II according to the activation energy required to disrupt the connection [18]. Further hygrothermal aging may result in a disruption of the chemical bonds, called hydrolysis, that causes permanent physical and chemical negative effects on the material (i.e., crazing and leeching) [19].

2.3 Dynamic Mechanical Analysis

Dynamic Mechanical Analysis (DMA) testing allows the measurement of the viscoelastic properties of the material by testing it as a function of temperature or time. By applying small oscillating displacements, the sample will deform according to its stiffness, and since it is done in a sinusoidal manner, it is possible to measure the response of the material in the viscoelastic range. This can provide information about stress and strain relaxations, in many cases regarding primary and secondary transitions as function of temperature (T_g).

DMA reports complex modulus and phase angle, E^* and δ respectively, in the form of storage modulus, or in-phase component, *E'* which denotes elastic behaviour and loss modulus or out of phase component, *E''* which denotes viscous or damping behaviour. The following equations relate the different reported values, where σ_0 is the maximum stress and ε_0 is the strain at the maximum stress [20].

$$E^* = E' + iE'' \tag{2.14}$$

$$E' = \frac{\sigma_0}{\varepsilon_0}\cos\delta \tag{2.15}$$

$$E'' = \frac{\sigma_0}{\varepsilon_0}\sin\delta \tag{2.16}$$

The magnitude of the complex modulus can be reported as a single real quantity in the form of:

$$|E^*| = |E'^2 + E''^2|^{1/2} \tag{2.17}$$

The ratio of energy lost to energy stored is defined as *tan δ,* which is related to the damping property of the material that describes the state of the material according to temperature and frequency [21].

$$\tan\delta = \frac{E''}{E'} \tag{2.18}$$

In this work, a quasi-static testing where a film tension test clamp is used with the DMA was applied at the standard frequency of 1 Hz. The machine measurements allow for the calculation of elastic modulus based on the measured stiffness (K_s), length and cross-sectional area by using the following equation [22]:

$$E = K_s\frac{l}{A} \tag{2.19}$$

2.4 Review of Relevant Work

A review of the literature revealed a vast volume of papers on testing of epoxies under various moisture and temperature conditions. Here, the most relevant research articles that will advance the understanding and assist in the development of the methodology and experimental procedures for this work are reported.

Evaluation of the elastic modulus of a polymer in the presence of water was carried out by Nogueira et al. in 2001 [12]. In that work, epoxy resin based on tetraglycidyl diaminodiphenylmethane and a novolac glycidyl ether resin was studied on the DMA, which highlighted the material's sensitivity to water in the viscoelastic range, showing a slightly bell shaped elastic modulus behaviour during initial water uptake. Their study was focused on the effects of samples immersed in water at various temperatures in three-point bending-loading configuration, cured at three different regimes.

LaPlante and Lee-Sullivan (2005) [23] studied the effect of moisture in a specialized structural film adhesive FM300. This paper shows the stress relaxation behaviour and fracture toughness on the material, due to hygrothermal aging, when plasticized. They reported that higher levels of water uptake yielded increased strength and rigidity. Another important conclusion was related to the load levels and loading rates – these test parameters significantly affected the determination of plasticization effect.

Lin and Chen (2005) [1] studied the effect on mechanical behaviour of sorption and desorption on a DGEBA/DDA (dicyandiamide) epoxy system by using molecular dynamics simulation. Elastic modulus and tensile strength data showed a reduction in value as exposure time increased. This paper also reported the relevance of hygrothermal history and specimen thickness.

Clancy et al. (2009) [24], developed molecular modeling calculations in order to analyze the changes in mechanical properties of DGEBA/DETDA (diethyltoluene diamine) as function of crosslinking degree, moisture content and temperature. They showed that elastic modulus has inconsistent behaviour as a result of water uptake, especially when compared to crosslinking and hygrothermal effects.

Ferguson and Qu (2006) [25] studied the effects of hygrothermal aging on the elastic modulus before and after drying an undisclosed type of epoxy underfill sample. Their testing was done at a single temperature (85 °C) combined with four different relative humidity conditions. They concluded that the effects of water were not very prominent during the initial stages of the condition but the degradation of the modulus was much higher during the later parts of the study; thermal aging by itself did not seem to have an effect on the elastic modulus.

Research on DGEBA/TETA at room temperature and 70% RH aging has been carried out by d'Almeida et al. (2003) [3]. In this work different hardener to resin mix ratio were tested for six months and the objective was to find its effects on stress and strain. It was found that the stoichiometric ratio of 13 phr showed higher tensile stress and strain than the other samples even after six months.

Papanicolaou et al. (2005) [9] studied a similar composition (DGEBA/DETA) in non-stoichiometric ratio by immersing the samples in water at 60 °C and 80 °C up to 1536 h. They reported the variation of T_g, *tan* δ, bending modulus and strength. It was noted that water absorption had a very small effect on the storage modulus. Similarly, Ivanova et al. (2001) [6] analyzed the effects of hydration in a rubber modified DGEBA/dicyandiamide material by immersion in water at 65 °C, reporting no significant variation of storage modulus in the glassy state.

Loh et al. (2004) [26] modelled the anomalous moisture uptake on an epoxy toughened adhesive by using a dual stage profile. The samples were exposed to different relative humidity conditions, including immersion in water which resulted in a better fit to the Fickian model especially for those samples with thickness of 2 mm. These samples also observed mass gains 20% higher than thinner samples that had been exposed to the same condition. Among suggested causes for this behaviour were the presence of voids, residual stresses and boundary layers as well as the shorter "boundary path" on the thinner specimens.

Zhou and Lucas [18] after studying DGEBA/mDPA and TGDDM/DDS for 1530 hours under immersed conditions at different temperatures proposed that there are two types of hydrogen bonding that occur in immersed samples: Type I and Type II. Type I indicating single hydrogen bonding (nearly-free water) which causes plasticization and Type II referring to double-bonded hydrogen bonding (tightly-bonded) which attaches to the backbone and causes a stiffening of the epoxy network. These findings highlight the importance of the interaction of hygrothermal history and sorbed water in the material.

Chapter 3
Molding Techniques and Experimental Methods

This chapter will first summarize the preparation techniques, including molding methods, used to fabricate samples according to specifications, and then present the experimental methods applied to characterize material behaviour as a function of hygrothermal exposure.

3.1 Material

The epoxy material used in this study is a DGEBA/TETA resin, comprised of highly pure diglycidyl ether of bisphenol-A (DGEBA, DER™331) hardened with triethylenetetramine (Ancamine® TETA) mixed in parts by weight 100:13. DGEBA/TETA resins are highly crosslinked polymers that have a wide array of industrial application as adhesives, encapsulating material, and as matrix component for composites. Physical properties of DGEBA and its chemical structure can be found in Table 3.1 and Figure 3.1 respectively. The epoxide equivalent weight, the viscosity and density are the most important parameters in this research.

Table 3.1. Typical properties of DER™331 [27].

Property	Value
Epoxide equivalent weight (g/eq)	182 – 192
Epoxide Percentage (%)	22.4 – 23.6
Functionality (eq/mol)	2
Epoxide Group Content (mmol/kg)	5200 – 5500
Dynamic Viscosity @ 25 °C (mPa•s)	11000 – 14000
Hydrolyzable Chloride Content (ppm)	500 Max.
Water Content (ppm)	700 Max.
Density @ 25 °C (g/ml)	1.16

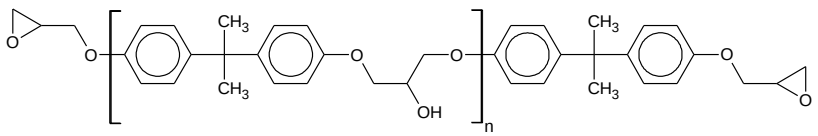

Figure 3.1. Chemical structure of DGEBA [28].

The TETA is a commonly used aliphatic amine for the curing of epoxies. Table 3.2 shows the most relevant properties of the specific TETA used.

Table 3.2. Typical properties of Ancamine® TETA [29].

Property	Value
Viscosity @ 25 °C (cP)	20
Amine value (mg KOH/g)	1435
Density @ 25 °C (g/ml)[a]	0.983
Equivalent weight (1/{H})	27

[a] Converted to SI units.

Likewise, its chemical structure is in Figure 3.2.

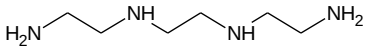

Figure 3.2. Chemical structure of TETA [30].

This epoxy-amine resin results from the reaction between the epoxide groups present in the DGEBA and the primary and secondary amine groups in the TETA (Figure 3.3). The secondary hydroxyl groups formed are the responsible for autocatalyzing the reaction [31]. According to the product datasheets [27, 29], the mix viscosity of DGEBA/TETA at 25 °C is 2250 mPa·s and the gel time for 150 g of the mix is approximately 30 minutes at 25 °C.

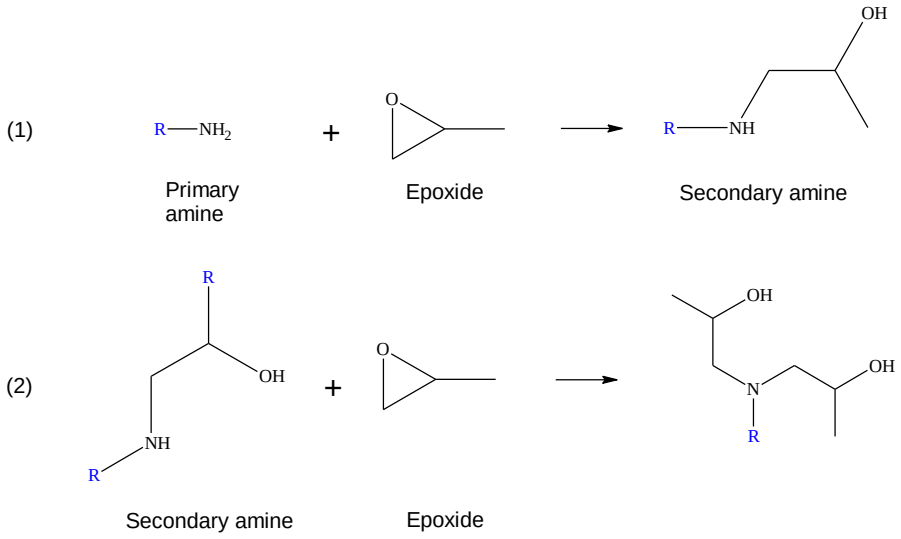

Figure 3.3. Typical epoxy-amine reaction in order: (1) and then (2).

3.2 Sample Fabrication

A major challenge in specimen preparation for dynamic mechanical testing is to achieve high quality, void free, thin and flat samples of epoxy. Voids occur because of entrapped bubbles that are inherently formed from pouring and mixing of the epoxy resin and hardener. As a result of the large number of samples needed for this experimental work, the determination of batch size was also critical to achieving good control of viscosity and cure time of the resin.

A major part of the experimental work was to develop a molding method to consistently obtain epoxy samples with dimensions 30 mm x 5 mm x 0.55 mm, within acceptable tolerance for DMA testing. As far as the author is aware, there are no references in the open literature with clear instructions to achieve this. These dimensions were selected to be within the DMA dimensional sample tolerance in the tension film clamp [22] and ASTM D882-12 guidelines [32]. Thus, significant effort was expended to study the literature in detail, including existing methods and their applicability to our needs. Among the major challenges were the very thin specimen requirement and the high viscosity of the material (and its consequences on bubble formation).

A number of fabrication techniques were attempted. Among the first was a custom-designed spin casting method. This method is widely used in industry and is known to minimize bubble reduction and dimensional variation but it requires the design and manufacturing of specialized molds able to withstand high centrifugal forces. Great care was taken to design and select mold materials that would allow the sample be easily released after spinning. Several prototypes were developed and tested, after revising and improving early iterations from practical experience. Unfortunately, it took too long to assemble and disassemble the mold together and the material life expectancy was relatively short. Specifically, the threaded holes of the mold and the mold itself tended to deform and creep with each use. It was concluded that this method would be too impractical in the longer term as we needed to mold at least 200 samples.

Eventually a different approach, which combined elements of spin casting and die casting, was developed and used. The combined approach yielded very good results. Both methods are described in more detail in sections 3.3.1 and 3.3.2 below.

For the purpose of this thesis, a sample is considered of acceptable quality if it satisfies the following conditions:

- Adequate dimensional tolerance (especially, thickness uniformity with relative standard deviation equal or lower to 0.035 mm) between batches and within the sample.
- Relatively smooth surface roughness.
- Few void formations, no visible cracks or imperfections.

Consequently, when designing the mold, the key parameters taken into account were:

- Leaks: Must be controllable so that material loss is minimized (or mitigated).
- Rigidity: Material must be rigid enough so that the cured resin maintains the dimensional stability required.
- Interaction mold-cast: As low as possible so that it allows for easy de-molding. Epoxy resin is highly polar, so a non-polar material such as polytetrafluoroethylene (PTFE) is suitable.
- Life expectancy: The mold must be reusable to fabricate over 200 samples over the duration of the experiments (3 to 5 months).
- Temperature limits: Must resist at least 130 °C (curing temperature of the resin).

3.3 Evaluation of Molding Techniques

3.3.1 Spin Casting

One particularly relevant study on the spin casting method was published by Mazzeo et al. [33] in 2011 which reported observations on bubble removal of thermosetting silicone polydimethylsiloxane (PDMS) – a resin with similar properties to DGEBA/TETA resin. By applying knowledge of buoyancy and bubble dissolution, they created a simulation capable of predicting a relationship between spin times and speed with bubble size. This method was taken into consideration during mold design in this work.

Additionally, in this work the spin casting method was adapted for use in a standard centrifuge machine. This meant that the mold size and mold weight had to be designed to fit within the Eppendorf centrifuge instrument model 5430 [34] outlined as:

- Mold Size: Able to fit in a 50 ml centrifuge vial.

- Mold weight limit: Less than 110 g (including centrifuge vial, lid and centrifuge adapter).

The proposed mold had to be assembled and placed into the centrifuge vial already fitted with the silicon rubber. Once placed within the vial, it had to be filled with epoxy by injection (through a slot at the top of the mold center) and centrifuged for a predetermined speed and time, before being separated from the centrifuge vial and cured in an oven. The curing temperature is 130 °C, which is outside the working temperature of polypropylene centrifuge vials.

The spin casting mold consisted of three PTFE sheets joined together by flat head countersunk screws, as shown in Figures 3.4 and 3.5 (see Appendix B – Drawings). Silicone rubber, formed with a template core, was added as a support and to act as an interface between the PTFE and the internal walls of the centrifuge vial. This setup was designed in such a way that the centrifugal forces would not affect the structural integrity of the mold and the presence of bubbles in the epoxy resin would be minimized.

Among the challenges of this type of three-part mold is the risk of leakage, mainly in two operations: (1) while centrifuging; and (2) while oven curing. During centrifuging, the combination of the vial and silicone rubber with the mold led to a tight fit that prevented leakage, but leakage would still occur during curing. Despite PTFE's excellent chemical resistance, its softening temperature range is relatively low (~130 °C), resulting in leaks. Thus, fabrication was modified from a single step-cure to a two-step cure: an initial step at 70 °C for 1 hour inside the centrifuge vial and a second step at 130 °C for 2 hours with the samples outside the mold.

While the mold worked very well during the initial runs, PTFE creep became excessive around the countersunk holes and the top part of the mold due to centrifuging and temperature cycling from 25 °C to 70 °C. This mold was then redesigned slightly where the bolts were changed to pan head screws to counter the deformation of the PTFE, which extended the life of the mold remarkably; however, the PTFE structural integrity around the bolt holes did not hold. Further iterations of this design were considered, but due to increasingly financial and time costs, this method was considered not viable to meet the project's needs.

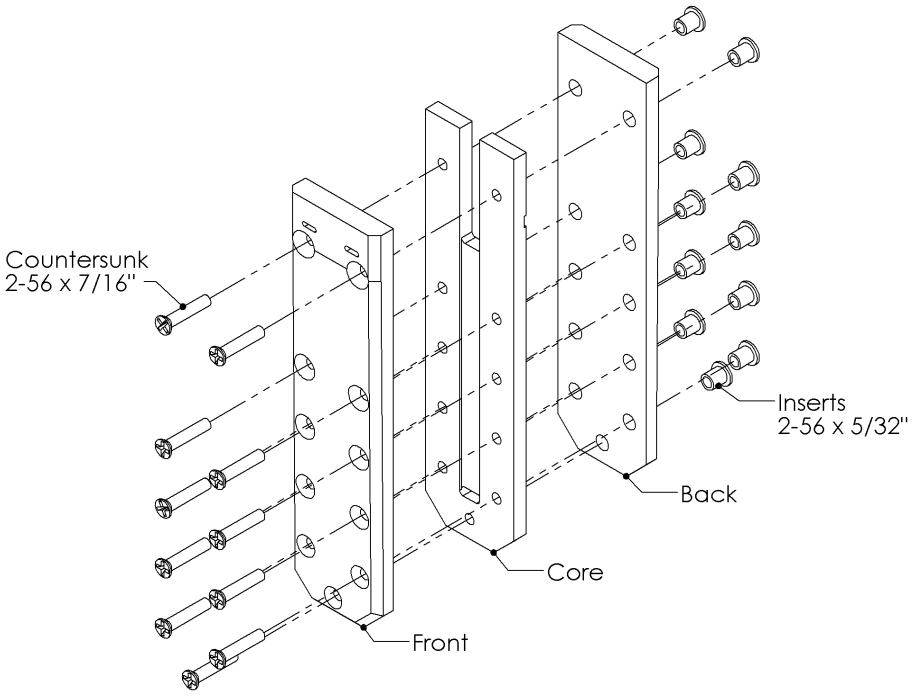

Figure 3.4. Centrifuge mold – Exploded view.

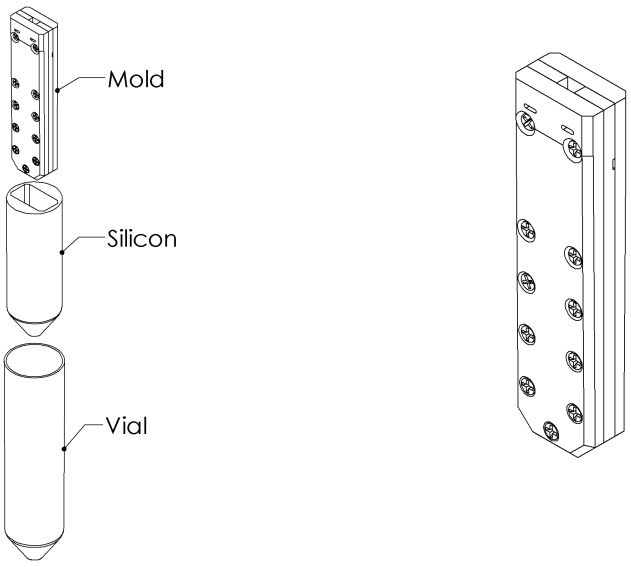

Figure 3.5. Centrifuge mold - Assembled views.

3.3.2 Die Casting

The mold design consisted of a thick sheet of specially prepared silicon rubber with a thin lid of the same material, both consisting of Freeman V-340 moldmaking silicon rubber with catalyst (CA45) mixed in a 10:1 weight ratio, cured initially for 12 hours at room temperature and then post-cured for 1 hour at 130 °C. This type of mold had the advantage of being easier to manufacture and thus replaceable when needed. The initial concerns involved the difficulty of getting good samples, but later this was remedied by controlling the fabrication process of the mold much more carefully. This two-part mold was maintained at a pre-heated temperature of 70 °C.

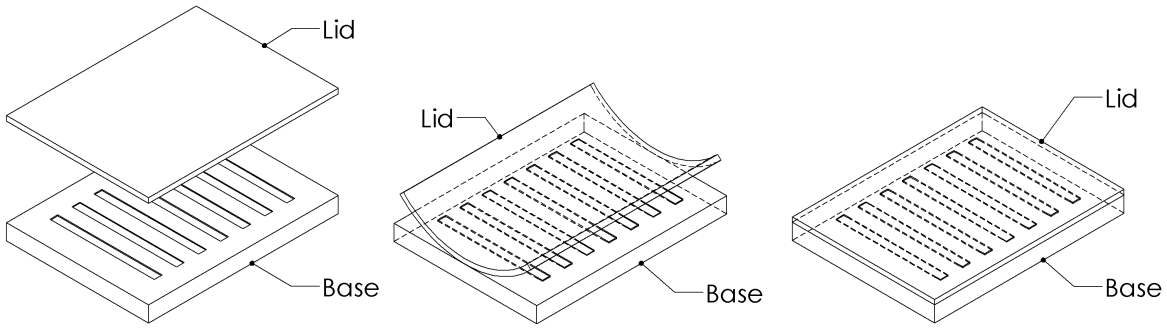

Figure 3.6. Assembly of the customized silicon mold, in order left to right.

The assembly and fabrication of the epoxy samples was much more straightforward: the epoxy mixture was to be poured into the mold base until it filled completely and uniformly. The lid was, thereafter, carefully placed on top of the mold with some weighted blocks to prevent air intake voids. Figure 3.6 shows the assembly of the mold.

3.3.3 Comparison of Sample Thickness from Molding Techniques

To evaluate the performance of the die casting method and the spin casting method, a t-test comparison of the standard deviation of the thickness (SD thickness) obtained along the sample length is shown in Table 3.3. Thickness measurements were taken at six different points along the length on each sample. A standard deviation was calculated per sample and used as the input value for the t-test comparison.

For a 95% confidence interval, the observed difference between the sample means is significant enough to reject the null hypothesis since the *t Stat* value 12.36 is not within the *t Critical two tail value*

(i.e. ±1.978). The spin casting method generates samples with tighter tolerance along the length with a standard deviation averaging 0.0091 mm, an improvement of 60% over the mean of the die casting method.

Table 3.3. t-test: two sample assuming unequal variances.

	Die Casting	Spin Casting
Mean (SD thickness)	0.023351127	0.009122551
Variance (SD thickness)	0.000186177	2.48172E-05
Observations	277	38
Hypothesized Mean Difference	0	
Degrees of freedom	133	
t Stat (SD thickness)	12.36004814	
P(T<=t) one-tail	3.8225E-24	
t Critical one-tail	1.656391244	
P(T<=t) two-tail	7.64499E-24	
t Critical two-tail	1.977961264	

For visual comparison, histograms of each molding technique are shown next (Figure 3.7 and Figure 3.8).

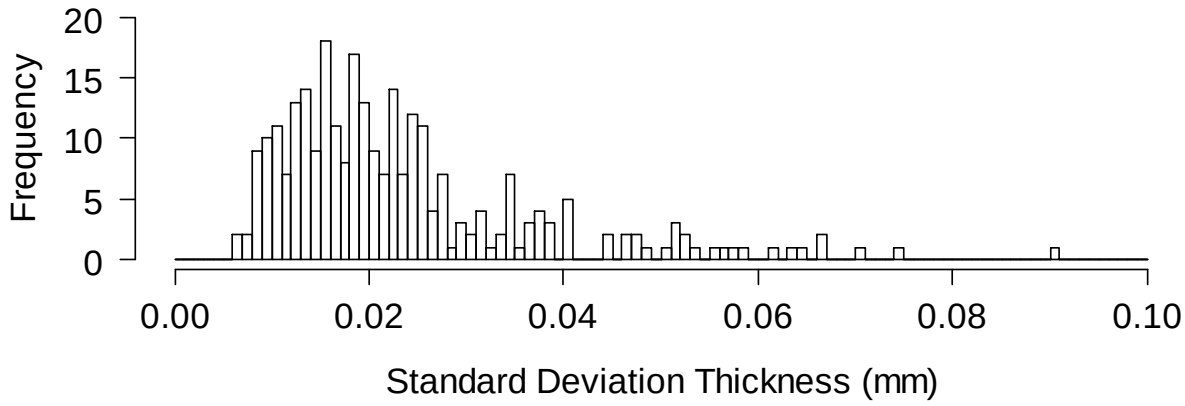

Figure 3.7. Die casting molding: Histogram standard deviation of thickness.

(Number of samples = 277. Bandwidth = 0.001 mm).

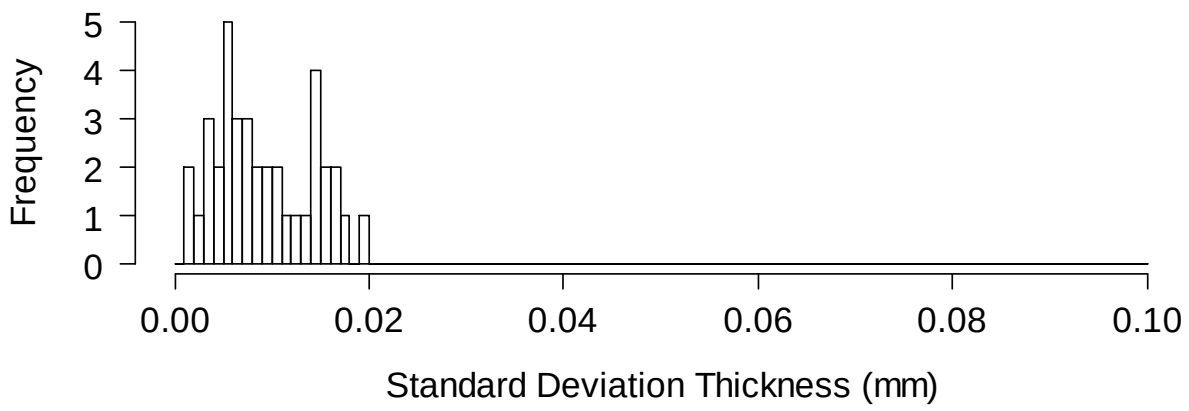

Figure 3.8. Spin casting molding: Histogram standard deviation of thickness

(Number of samples = 38. Bandwidth = 0.001 mm).

3.4 Sample Preparation

After considerable trial and error, the following specimen preparation technique was employed: batches of 5 g of DGEBA mixed with 13 phr of TETA relative to the resin were vacuum-degassed (26 inHg) while being vortex-mixed for roughly 5 minutes in a centrifuge vial. When the mixture was visibly homogeneous, it was centrifuged (Eppendorf 5430) for around 5 minutes at 5000 RPM, then poured into the two-part silicon rubber mold, pre-heated at 70 °C (±0.1 °C). The samples in the mold were cured for 1 hour at this temperature. After curing was complete, the samples were de-molded, cut and stored in plastic bags. Each batch yielded 14 samples with dimensions 33 mm x 5 mm x 0.55 mm and average initial mass of 105 mg. The average sample thickness was calculated by using at least six micrometer-measured points, selecting the ones with a thickness standard deviation lower than 0.035 mm. These samples were later post-cured at 130 °C for 2 hours to ensure reaching the final T_g with a complete cure. The appropriate curing time and temperature were determined using Differential Scanning Calorimetry (DSC) following the ASTM E2602-09 [35]. The DSC results can be found in Appendix A.

3.5 Experimental Methods

To study the progressive effects of hygrothermal exposure on material properties, DMA film tension tests were performed on specimens subjected to three exposure conditions: unaged; dry, thermally aged; and hygrothermally aged. The combinations of temperature and relative humidity (RH) conditions are shown in Figure 3.9. Sample conditioning and DMA testing were conducted in parallel in the Advanced

Composites and Adhesives Lab at the University of Waterloo and in the Materials Lab at Blackberry Ltd. In addition to DMA film tension tests, gravimetric analysis was also conducted for the same set of hygrothermally aged samples to determine the diffusion coefficient. Sections 3.5.3 and 3.5.4 explain the procedures in more detail.

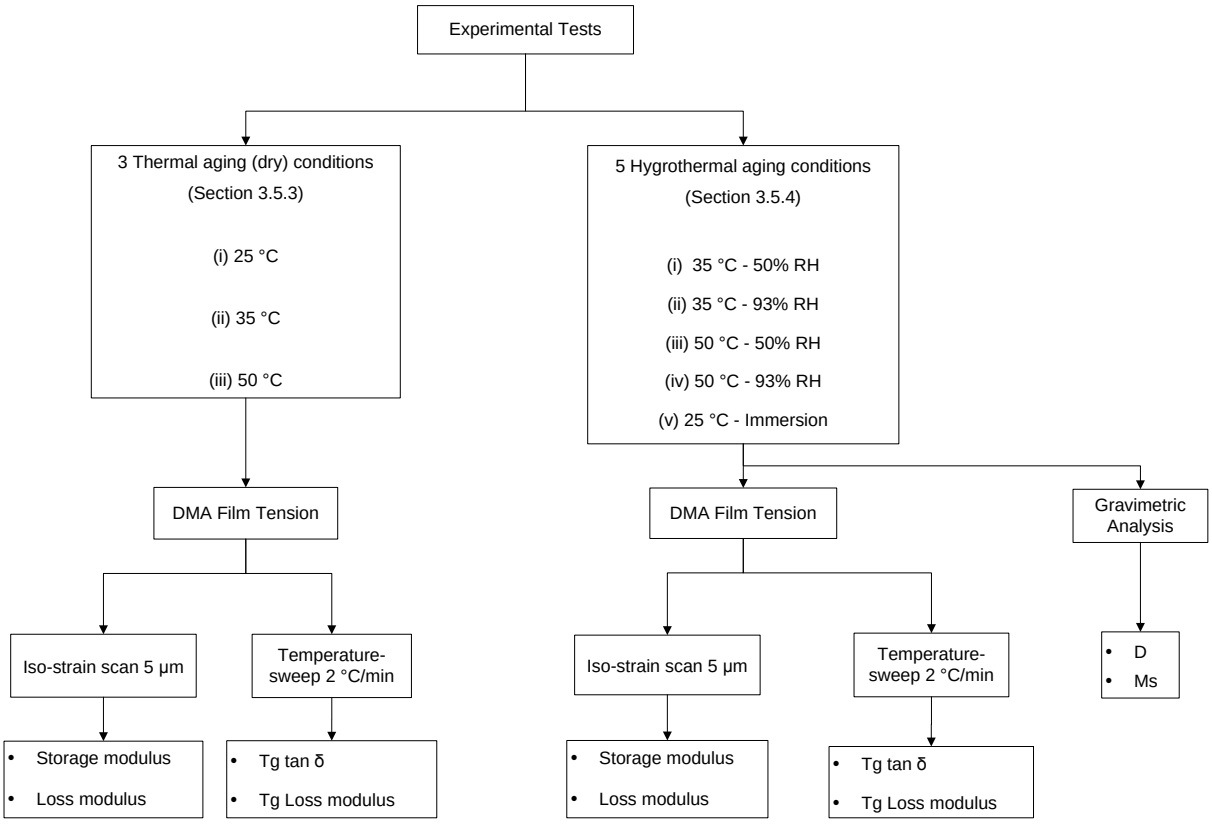

Figure 3.9. Schematic diagram of the exposure conditions and tests performed.

3.5.1 Specimen Pre-conditioning

To establish a reliable baseline, samples were pre-conditioned in a vacuum oven (model VWR 1430M) at 130 °C for 30 minutes to induce thermal rejuvenation [36] and to dry out any moisture introduced during sample preparation. They were then dry-weighed to within 0.1 mg resolution (Sartorius CP124S) and measured before being placed in the desiccator for 48 h.

3.5.2 Dynamic Mechanical Analyzer Testing

The tests were performed in the film tension mode [22] of the DMA instrument (TA instruments Model Q800) because this mode enables testing of thin samples. At the outset, it was necessary to have thin specimens since the DMA machine has a very limited load of 15 N and it would allow moisture equilibrium to be attained in a reasonable time. The specimens were tested in the linear range of material response, with oscillation amplitude of 5 μm at room temperature (25 °C), adjusted torque of 3 in-lbs, at a frequency of 1 Hz, a static force of 0.0100 N to prevent buckling and force track of 125%. The nominal specimen dimensions were 33 mm x 5 mm x 0.55 mm with an average gauge length of 12.75 mm (±0.25 mm) as shown in Figure 3.10.

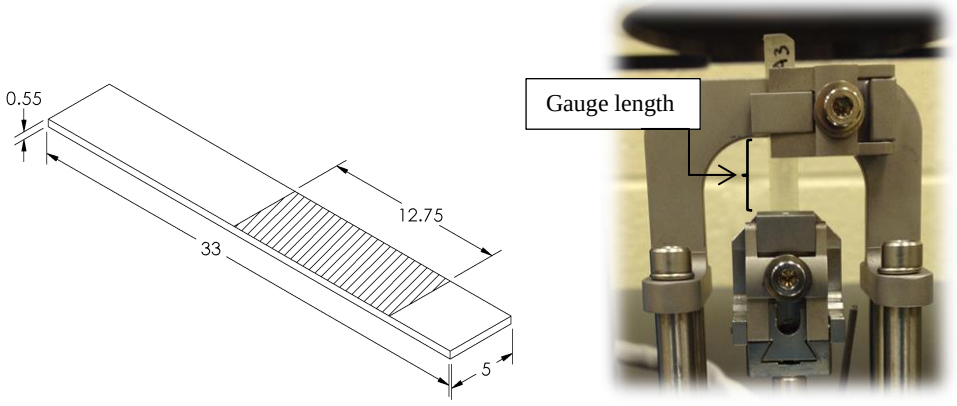

a) b)

Figure 3.10. a) Sample dimensions and gauge length (mm), and b) Mounting on DMA instrument.

An initial experiment found that the measurement stabilization commonly occurs at around 7 minutes, thus this was the point at which the property measurements were taken for all samples. Since storage and loss moduli can be highly variable in polymeric materials, we selected samples with initial storage modulus within 5% relative standard deviation (i.e., storage modulus ranging from 2140 MPa to 2600 MPa, average of 2384.7 MPa and standard deviation of 116.35 MPa). The histogram in Figure 3.11 shows that approximately 70% of the tested samples met the storage modulus criteria.

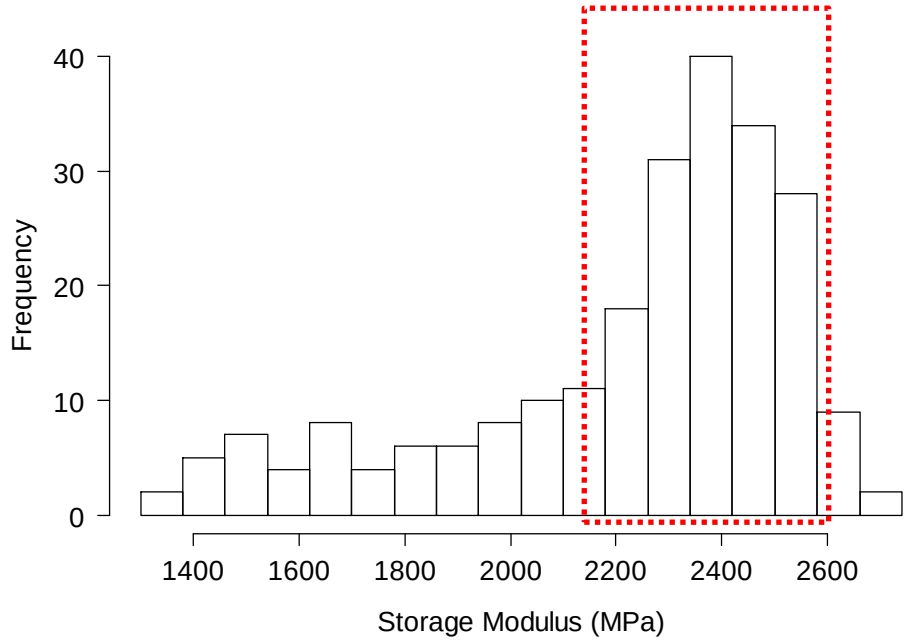

Figure 3.11. Histogram showing the range of storage moduli for all tested samples

(Number of samples = 233. Bandwidth = 80 MPa).

3.5.3 Thermal Aging

To study the effects of short and long term exposure to sub-T_g temperatures on the storage modulus and loss modulus, samples were exposed to three different isothermal conditions: (i) 25 °C, (ii) 35 °C, and (iii) 50 °C. As highlighted by researchers [12, 25] who have worked on other epoxy types, these temperatures are not expected to have any significant effects at short term exposure. However, some significant effects might be noticed later in the process (long-term exposure).

At each temperature condition, the samples were held on a custom-made polycarbonate rack (Figure 3.12) placed inside sealed 1 litre containers filled with anhydrous calcium sulfate (Drierite™) desiccant to keep them dry during their conditioning.

The recommended desiccant amount of 4 oz desiccant per 10 ft^3 of free volume to dry the air in the container was used [37], which converts to about 0.4 g/L. Because the container was planned to be opened multiple times to retrieve the materials, a good amount of desiccant was needed to ensure dry samples at all times. It was decided that 100 g of desiccant was needed per container to aim for a factor of safety of around 250.

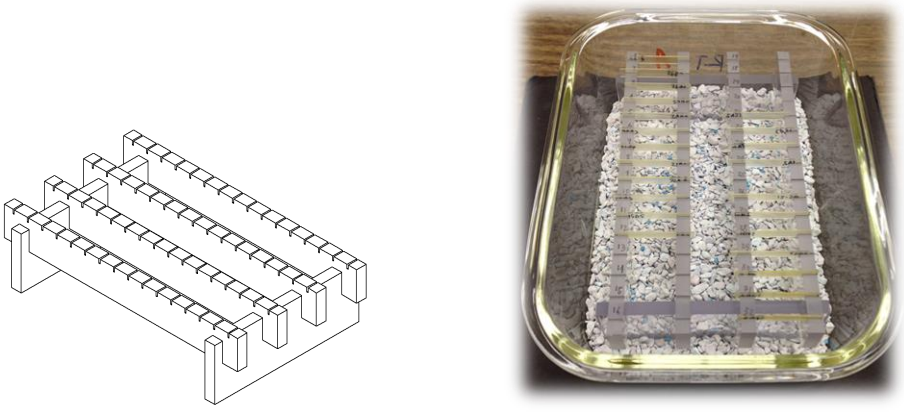

a) b)

Figure 3.12. a) Custom-made polycarbonate rack design, b) Samples placed on rack.

Sampling was conducted daily for the first 7 days, and then weekly until the 55th day for a total of around 1320 hours of exposure.

The procedure involved working with 12 samples per condition (i.e., 25 °C, 35 °C and 50 °C, respectively) in the following way:

- During the initial period of higher sampling, three samples (for one data point) were removed from the chamber and allowed to reach room temperature in a desiccator.
- Each sample was then weighed using an analytical balance with a precision of 0.1 mg (Sartorius CP124S), tested on the DMA and finally returned to the oven. To check whether or not briefly removing the sample from the chamber for DMA testing had an impact on test results, a consistent procedure was applied. For each sample set of three to obtain one data point, only two previously tested specimens were selected plus a new sample was added. This confirmed that variation was not a result of specimen handling.

Beginning mid-way through the experiment, and when all 12 samples had been tested at least once, seven replicates from the 12 were selected and repeatedly subjected to DMA to study any potential variation in more detail in the most critical phase.

Additionally, on the 100th day (around 2400 hours) a temperature-sweep test was conducted on a new untested three-sample set. This test was done from room temperature to 180 °C at 2 °C/min to determine the T_g by loss modulus and *tan* δ, as well as the storage modulus on the whole temperature range.

3.5.4 Hygrothermal Aging and Moisture Uptake

The hygrothermal test conditions were selected based on the literature review and the IEC 60068-2-78 standard [38].

Samples were subjected to five different hygrothermal conditions: (i) 35°C-50% RH; (ii) 35°C-93% RH; (iii) 50°C-50% RH; (iv) 50°C-93% RH; and lastly (v) submerged in deionized water at room temperature (25°C-Imm). The first four conditions were tested in dedicated environmental chambers with the samples being held in place by custom-made polycarbonate racks (Figure 3.12). Samples in condition (v) were placed in another rack completely submerged in the liquid.

The sampling involved performing repeated gravimetric measurements and DMA iso-strain until samples had reached saturation at which point DMA temperature-sweep tests were carried out. At least three replicates were used in each case. To perform measurements, samples were, in order:

- Removed from the environmental chamber;
- Wiped carefully with a lint-free tissue paper;
- Weighted using an analytical balance with a precision of 0.001 mg (higher resolution than the thermal aging study);
- Cooled to ambient temperature;
- Tested on the DMA and;
- Returned to their exposure condition.

The weights of the samples taken every two weeks were used to determine when saturation had been reached. According to the ASTM D570-98 [39], the average of the difference of the last three measurements should be less than 1% of the total mass uptake, for the samples to be considered saturated.

When all the specimens had reached saturation, a DMA temperature-sweep test was applied to find the influence of the aging on the storage modulus, loss modulus and *tan δ*. The ramp-up was done at 2 °C/min from room temperature to 180 °C.

Dow Corning high-vacuum grease was used to coat the sample to prevent moisture loss when tested to determine T_g [23, 40]. Care was taken to ensure it did not affect the T_g in a measurable way.

Chapter 4

Results and Discussion

This chapter presents and discusses the experimental results. First, the moisture uptake diagrams will be presented and followed by the effects of exposure time, moisture uptake and temperature, respectively on the material modulus. Finally, the influence of moisture and temperature on the epoxy T_g as indicated by both loss modulus and *tan δ* will be discussed.

4.1 Moisture uptake study

Following the conventional way of representing moisture plots, the square root of time was used on the x-axis in order to properly discern the initial linear mass uptake and determine the moisture diffusivity coefficient.

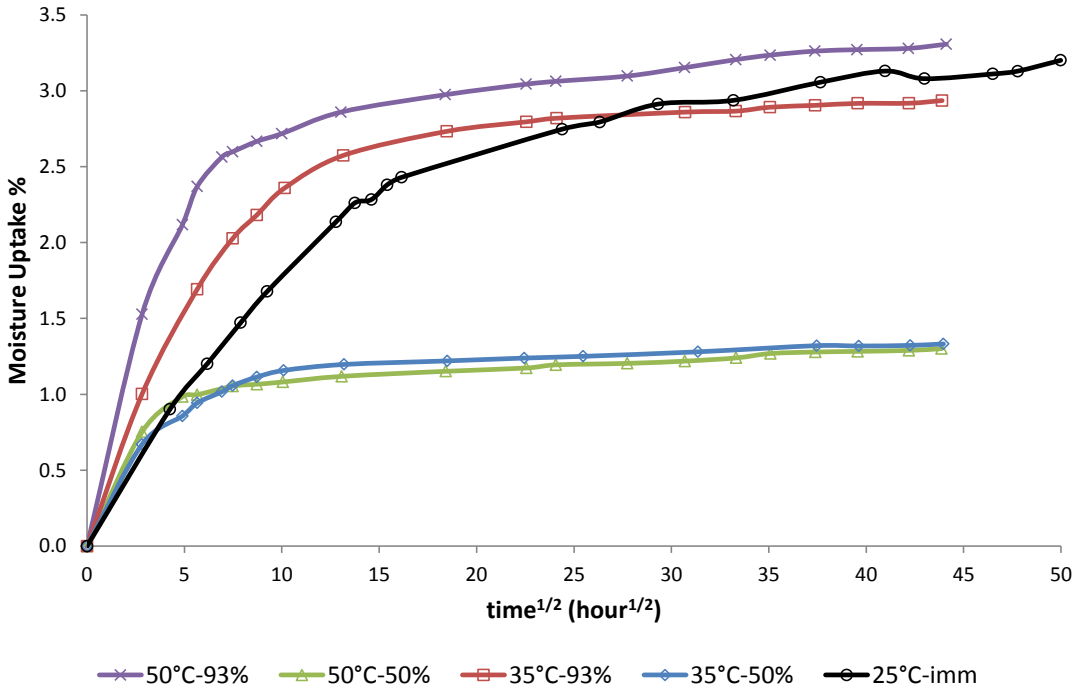

Figure 4.1. Moisture uptake data for hygrothermal and immersed conditions as function of exposure time.

Figure 4.1 shows the moisture uptake curve as a function of time for up to 2500 hours for the five different conditions (with a minimum of three samples per condition). Clearly, when the relative humidity

(RH) conditions are similar, i.e., 50°C-50% and 35°C-50%, the moisture update behaviour and mass saturation points are similar. At this relatively low humidity, the saturation points for both conditions are at 1.30% and 1.33%, respectively, and were reached in about 1600 hours. At these relatively low temperatures, the 15 °C difference had almost no effect. A further ANOVA test (Appendix C) confirms this hypothesis. This finding is consistent with the fact that molecular relaxations of the polymer are not strong far from the T_g (at least for the time period studied), and therefore, no significant differences are visible in the moisture curves.

The condition 50°C-93% observes the highest amount of absorbed water at 3.30%. The rapid water uptake is very evident as well. The curve shapes for samples at conditions 35°C-93% and 50°C-93% are quite similar, but the slopes of initial stage of absorption are noticeably different. The curves appear to separate after 600 hours. The condition 35°C-93% has a mass saturation point of 2.93%.

At low humidity levels, there is neither a measurable temperature effect nor difference in moisture uptake curve. When humidity increases, however, the temperature effect begins to take a more prominent role in moisture uptake behaviour, even though the temperature difference is only 15 °C. In other words, the role of temperature becomes more important when the RH is high. An ANOVA study (Appendix C) indicates that temperature changes from having no effect at low RH to having weak effects at high RH. This result suggests that high humidity triggers a temperature effect in the moisture uptake process.

As expected, samples that were immersed at room temperature (3.20%) exhibit very different moisture absorption curve. This curve starts below the 35°C-93% curve but slowly climbs up until it surpasses it, almost reaching the 50°C-93% curve. The absence of heat delays the water uptake, since molecular relaxation is not present. Heat expands the molecular network volume, inducing the polymer cross-linked structure to a transition into a rubbery-like state and accelerating moisture absorption during the initial part of the process.

Pulling together all the curves in Figure 4.1, it can be concluded that the combination of temperature and RH of the environment affects moisture diffusion into epoxy. In general, the rate of absorption is temperature-dependent, while the final equilibrium moisture uptake depends on the RH. This is consistent with other reports in the literature [16, 41].

4.1.1 Diffusion coefficient

The diffusion coefficient or diffusivity is calculated by assuming Fickian behaviour from equation 2.9. In addition, to consider the contributing factor of absorption through the edges (D_c) equation 2.12 must be used, which results in an approximate correction factor of around 0.7877. The original and corrected diffusion coefficient values are in Table 4.1 and plotted in Figure 4.2 along their respective standard deviations (SD).

Table 4.1. Diffusion coefficients obtained by Fickian model.

Condition	D (mm^2/h)	SD (mm^2/h)	D_c (mm^2/h)	SD (mm^2/h)	M_∞ %
25°C -immersed [a, b]	2.82×10^{-4}	1.14×10^{-4}	2.23×10^{-4}	0.89×10^{-4}	3.20
35°C-50% [c]	1.61×10^{-3}	0.11×10^{-3}	1.27×10^{-3}	0.08×10^{-3}	1.33
35°C-93% [c]	8.53×10^{-4}	1.70×10^{-4}	6.70×10^{-4}	1.37×10^{-4}	2.93
50°C-50% [c]	2.20×10^{-3}	0.21×10^{-3}	1.73×10^{-3}	0.17×10^{-3}	1.30
50°C-93% [c]	1.56×10^{-3}	0.13×10^{-3}	1.22×10^{-3}	0.11×10^{-3}	3.30

[a] Measured at 18 hours.
[b] Diffusion coefficient approximated for 25°C-immersed.
[c] Measured at 8 hours.

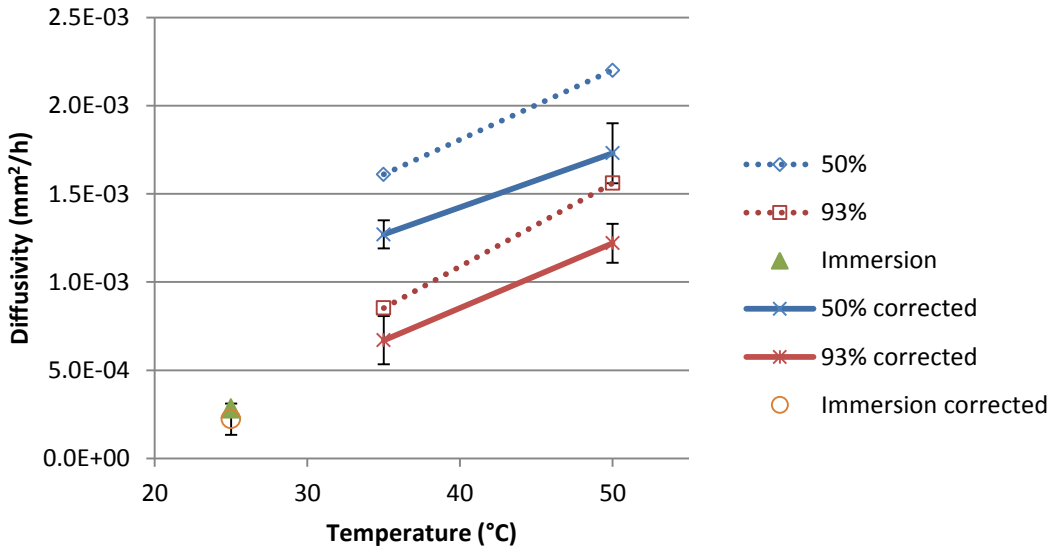

Figure 4.2. Diffusivity as a function of temperature and relative humidity.

In the literature, the theoretical basis for approximating a valid diffusion coefficient is by using the first 60% of the uptake curve if it is linear. From Figure 4.3 to Figure 4.6, the different hygrothermal conditions observed reasonable agreement with the first part of the Fickian fit ($M_t/M_s < 0.6$), but the model overestimates the mass update beyond that point. This suggests that the uptake behaviour at these specific conditions is non-Fickian in nature.

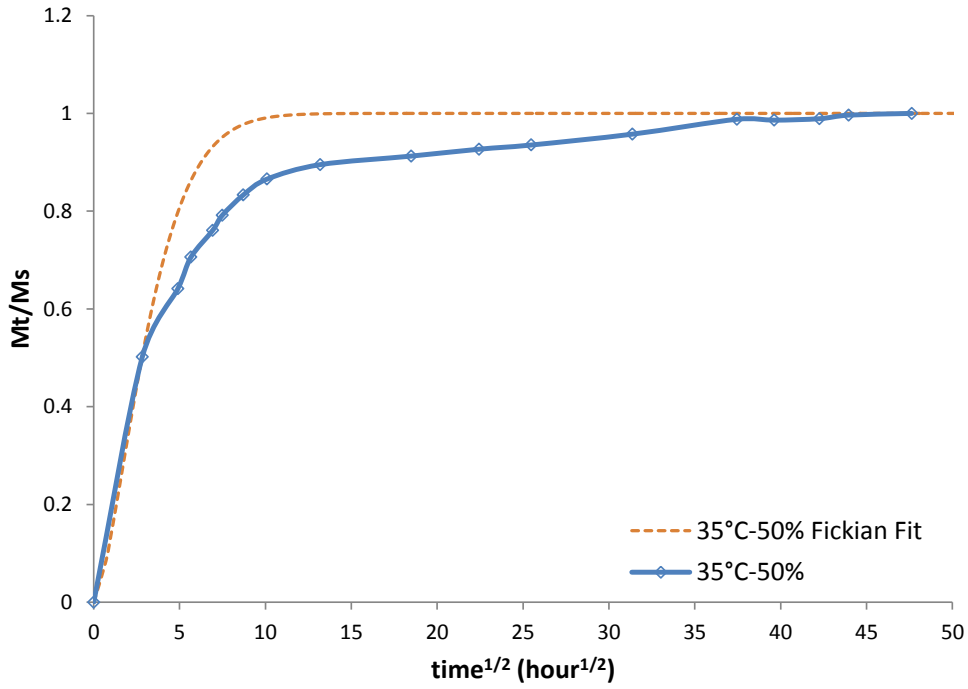

Figure 4.3. Absorption ratio and Fickian fit as function of exposure time: 35°C-50%.

Figure 4.7 shows fit evaluation of multiple diffusion coefficients to the experimental 25°C-imm curve. These coefficients are represented by the measurement at 18 hours (30%), average of the first 85 hours and measurement at 85 hours (50%), which corresponds to 2.82 $x10^{-4}$ mm^2/h, 2.08 $x10^{-4}$ mm^2/h and 1.64 $x10^{-4}$ mm^2/h, respectively. In this case, among the diffusion coefficients tested, the better fit appears to be close to 2.82 $x10^{-4}$ mm^2/h. However, the wider range of diffusion coefficients estimated within the region complicates the determination of a single reliable value. The open literature currently offers conflicting results on whether DGEBA/TETA systems have Fickian (or not) for immersed conditions [11, 42], but our tests tend to support non-Fickian diffusion.

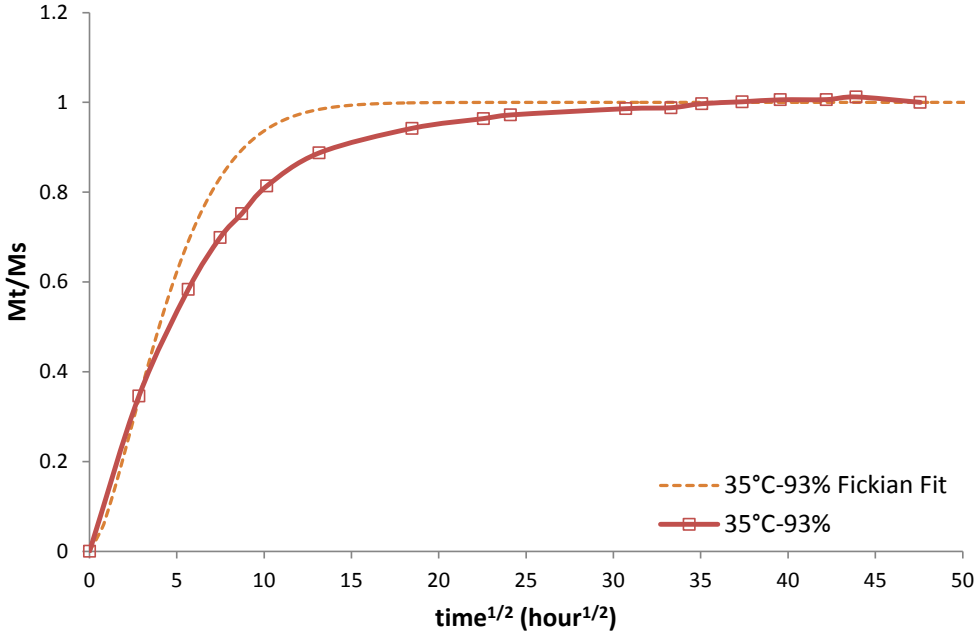

Figure 4.4. Absorption ratio and Fickian fit as function of exposure time: 35°C-93%.

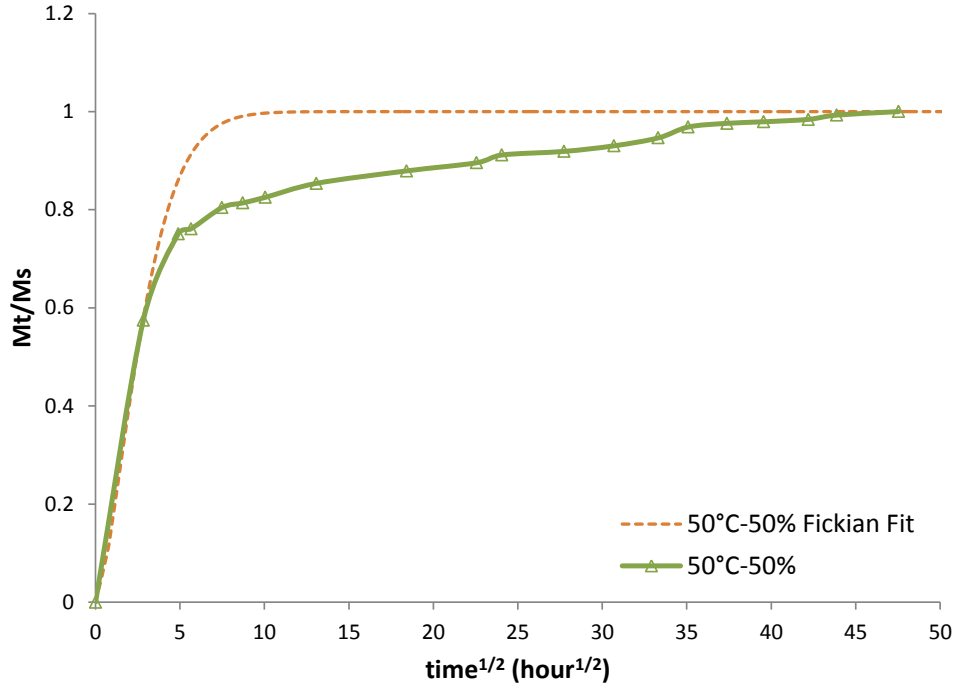

Figure 4.5. Absorption ratio and Fickian fit as function of exposure time: 50°C-50%.

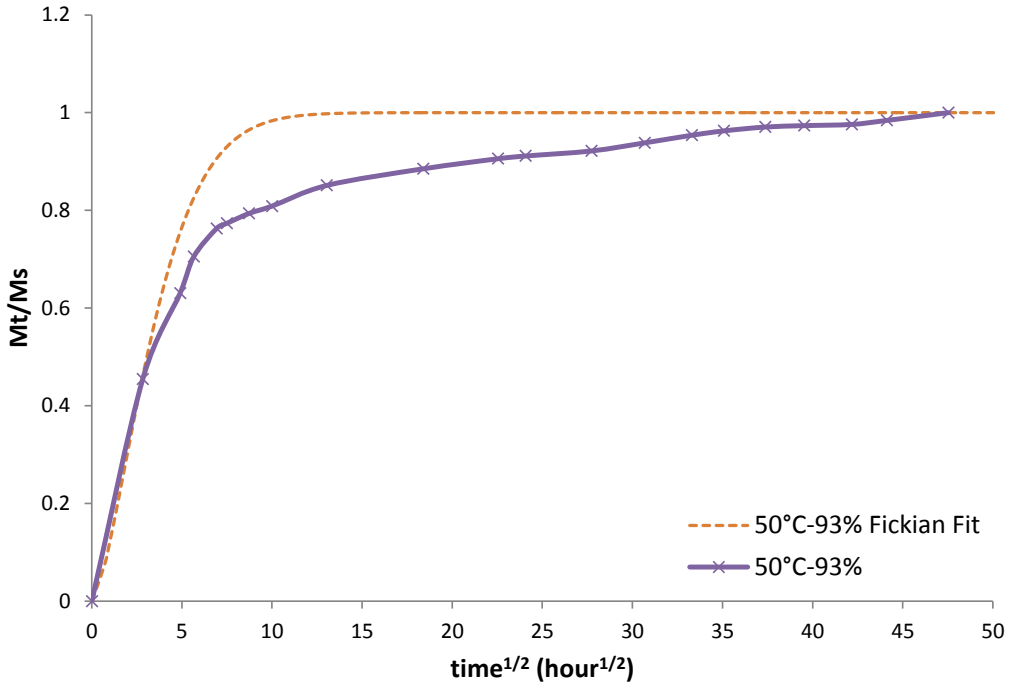

Figure 4.6. Absorption ratio and Fickian fit as function of exposure time: 50°C-93%.

Table 4.2 lists the boundary moisture concentration data. The data represents the maximum amount of moisture per volume of the material and is calculated by dividing the saturation moisture mass gain over the original volume of the specimen [4]. Thus, the boundary moisture concentration values are proportional to increases in mass uptake.

An analysis of the diffusion coefficients shows that higher diffusion coefficients are due to higher temperature exposure which is consistent with reports by other authors [16]. The temperature increases the specific volume and relaxes the polymer network which in turn creates more voids for the water molecules to fill in during the uptake. However, Pascault et al. [2] have suggested that the free volume, which depends on crosslink density and morphology, in polymers is only partly responsible for the water absorption during the initial phase.

On the other hand, if we maintain temperature and increase relative humidities, there will be lower diffusivity (i.e. 35°C-93% RH, 50°C-93% RH and 25°C-Imm). This is not readily intuitive; however, Soles and Yee [43] provide a plausible explanation that can be related to this phenomenon: the high polarity of the resin in the hydroxyl group generates trapping sites that interact with water and impedes its

transportation, which would naturally decrease the diffusion coefficient. This phenomenon would be mostly observed at higher humidities.

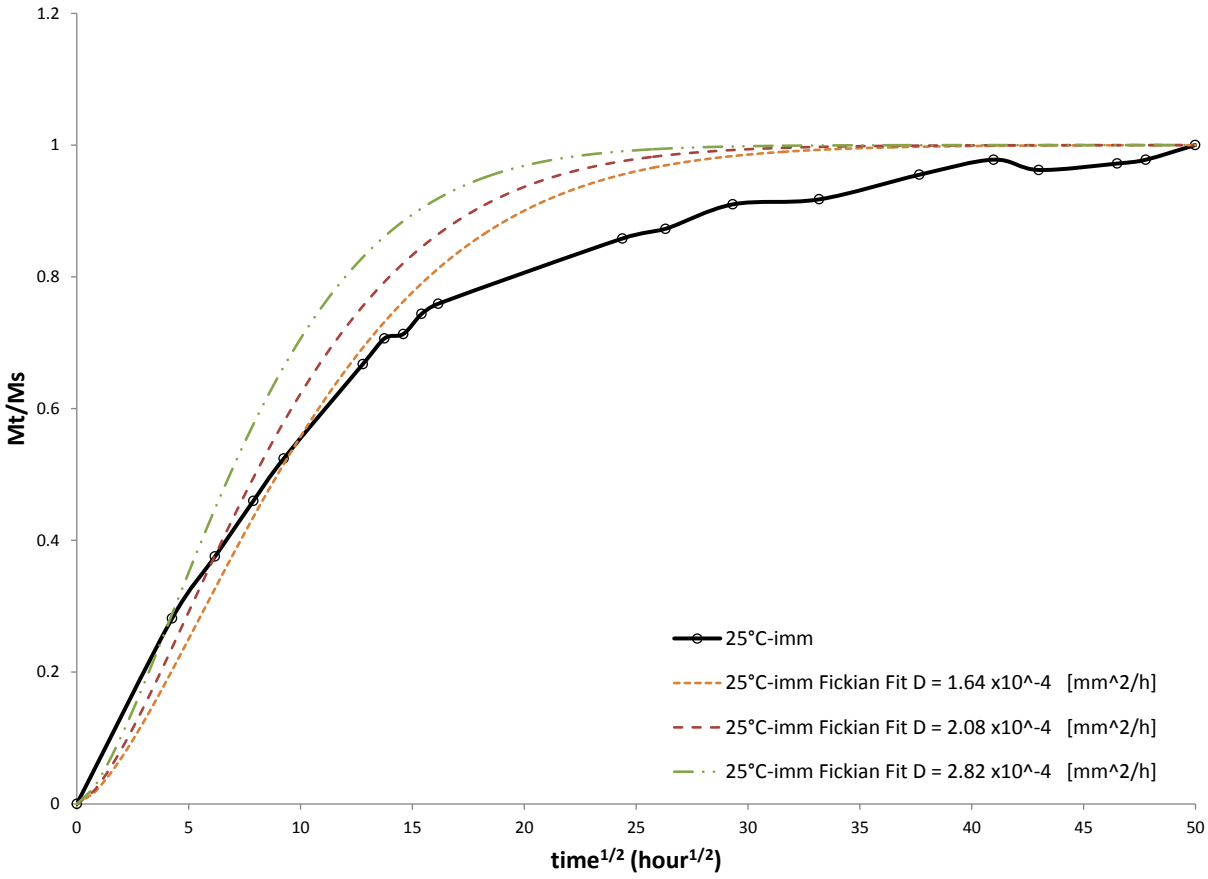

Figure 4.7. Absorption ratio and Fickian fit as function of exposure time: 25°C-imm.

Table 4.2. Boundary moisture concentration data.

Condition	C_∞ (g/mm^3)
25°C -Immersed	3.61 x10^{-5}
35°C-50%	1.53 x10^{-5}
35°C-93%	3.31 x10^{-5}
50°C-50%	1.50 x10^{-5}
50°C-93%	3.75 x10^{-5}

In addition, it is also clear that the behaviour is non-Fickian or anomalous for all the conditions tested. A non-Fickian approach is one where the relaxation rate in the polymer influences the uptake behaviour. Many researchers have developed different models to study this phenomenon ranging from time-varying diffusion coefficients [14], time-varying boundary conditions [44], and Langmuir two-phase interactions [45]. But for the purpose of estimating the coefficients of diffusion, a Fickian approach can be used since there is generally good agreement during the first 60% part of the uptake [14].

It is important to highlight that some researchers have noticed that samples' thickness is potentially influential when determining if behaviour is Fickian or anomalous. For instance, Loh et al. [26] noticed that epoxy samples above a certain threshold (in their case 2 mm) and exposed to higher humidities appeared to conform more accurately to Fickian model than those that did not satisfy these prerequisites. This behaviour is most likely the result of the constant surface concentration that the Fickian model assumes [46].

4.2 DMA results: Effects of time and moisture uptake

Two sets of dynamic mechanical analysis (DMA) tests were performed to evaluate viscoelastic behaviour due to prolonged hygrothermal exposure at the various conditions. In this section, the effect of exposure time on the storage modulus using an iso-strain test at room temperature will be reported. In the following section 4.3, the effect of temperature on the storage, loss moduli and *tan* δ parameters as tested using the temperature sweep will be shown.

The DMA storage moduli plotted as a function of square root of time up to 1320 hours (55 days) for the samples exposed to isothermal temperatures (i.e., dry conditions 25 °C, 35 °C and 50 °C) and hygrothermal conditions are shown in Figure 4.8 and Figure 4.9, respectively.

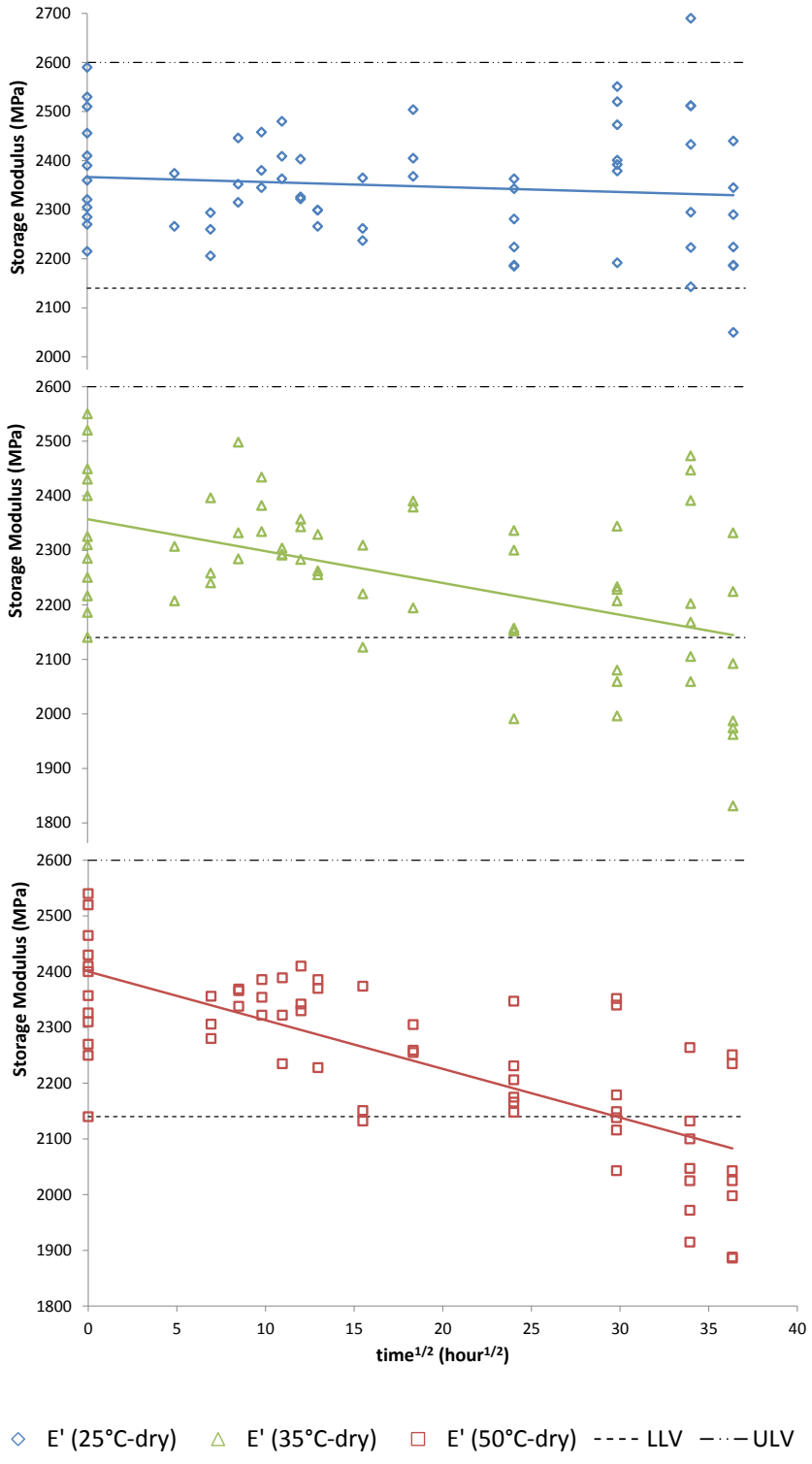

Figure 4.8. Storage modulus as function of exposure time: dry conditions.

In these graphs, the Upper Level Value (ULV) and Lower Level Value (LLV) represent the limits that were set in Section 3.5.2. Best fit lines representing the trends are shown as well.

Figure 4.8 shows the variation of the storage modulus as a function of square root of time. It is noted that samples kept at 25 °C observed no significant change which served as adequate control samples. However, samples exposed to 50 °C tend to suffer some loss in storage modulus with time, especially when compared to the other conditioned temperatures. This behaviour, when evaluated in a one-way ANOVA test per condition (Appendix C), suggests that there is a strong statistical significance of time on the storage modulus for samples exposed to 35 °C and 50 °C. The behaviour shown here contradicts the widely reported outcome of either minimal change or isothermal storage modulus increases during physical aging, due to decreased mobility of submolecular segments in some polymers (i.e., reduction of the specific volume between the cross-links) caused by temperature and time interactions [47, 48]. The results of the current research suggests that assuming 100% cure, different types of amine hardeners in epoxy-amine system may alter submolecular dynamics of the samples on the glassy state.

In addition, when evaluating hygrothermal response as function of exposure time (Figure 4.9), the storage modulus appears to remain constant, i.e., a different behaviour than observed for dry samples. It can be inferred that the interplay of heat transfer and mass uptake has a counter effect on any apparent drop in storage modulus. Some authors have conducted molecular simulations to model this behaviour and found that the interaction between temperature and the water content affects the system in different ways [24]: this may explain our observed increased modulus. The plot showing storage modulus as function of mass uptake (Figure 4.10) further supports this premise.

Table 4.3 highlights the results from a one-way ANOVA study conducted using statistical software, R Studio (See Appendix C for details) per condition to assess statistical ($p < 0.05$) and practical significance. Each asterisk represents a different level of significance, with a three-star level representing a “very significant effect” and one-star level a “not significant effect”; thus higher number of asterisks indicates stronger significance.

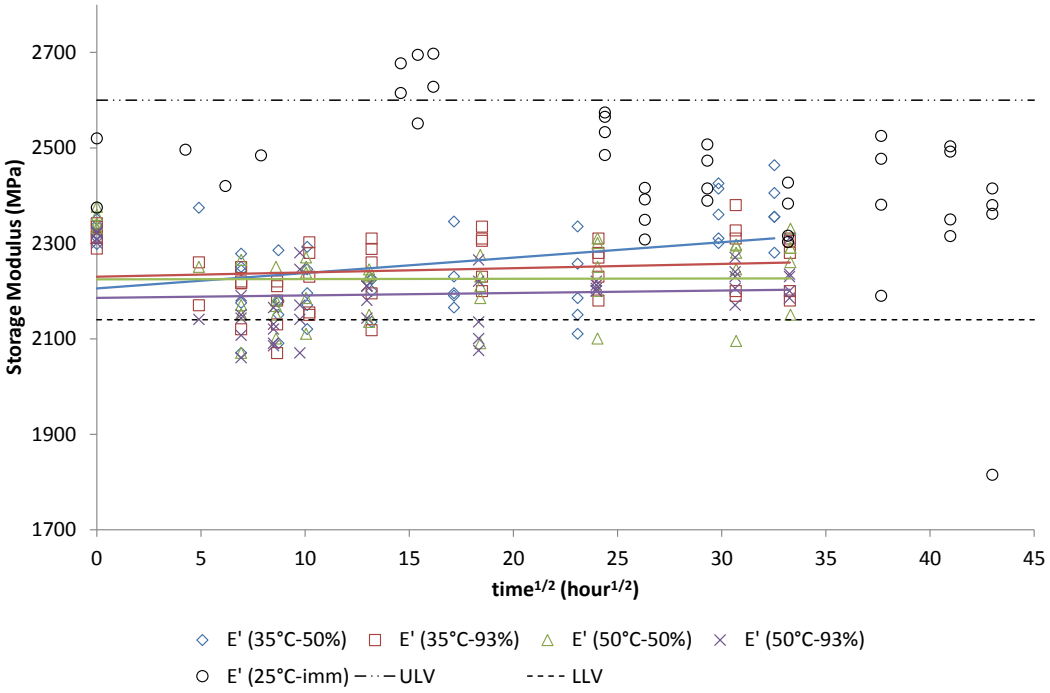

Figure 4.9. Storage modulus as function of exposure time for hygrothermal and immersed conditions.

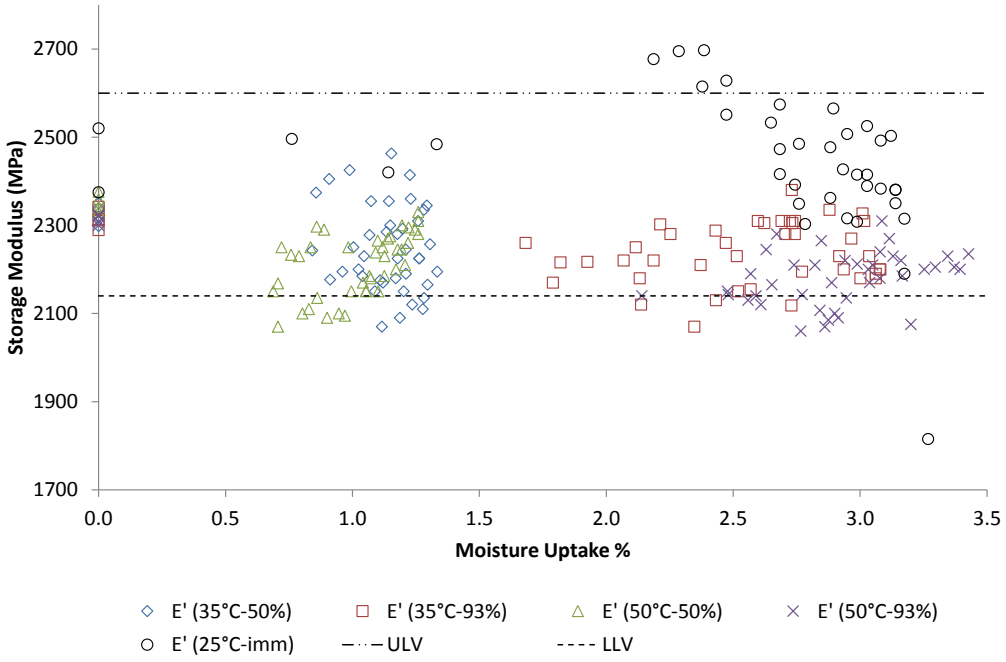

Figure 4.10. Storage modulus as function of moisture uptake for hygrothermal and immersed conditions.

Table 4.3. *p*-values for all condition E' vs $t^{1/2}$.

Temperature (°C)	Humidity (%)	*p*-value	Significance
25	0	0.38	
35	0	1.2×10^{-5}	***
50	0	2.1×10^{-12}	***
35	50	0.016	*
35	93	0.36	
50	50	0.96	
50	93	0.61	
25	imm	0.0023	**

In Figure 4.11, small differences between specimens maintained at dry conditions and immersed specimens at the same temperature (25 °C) can be observed – there are indications that the storage moduli for immersed samples are generally higher. However, when subjected to ANOVA no statistical significance was found: water immersion by itself does not seem to influence the storage modulus. Water participates as a plasticizer and initiates hydrogen bonding, thereby altering the flexibility of the backbone and introducing a new relaxation mechanism, but at room temperature, this relaxation is absent [49].

In Figure 4.12 , a cross-plot of storage modulus and mass uptake as a function of time is presented. This graph visualizes the relationship between the water uptake and the storage modulus during the rapid intake phase. Since the storage modulus is constant, there is no tangible link between these two parameters in this material for the condition listed. These results are consistent with those reported by Nogueira et al. [12].

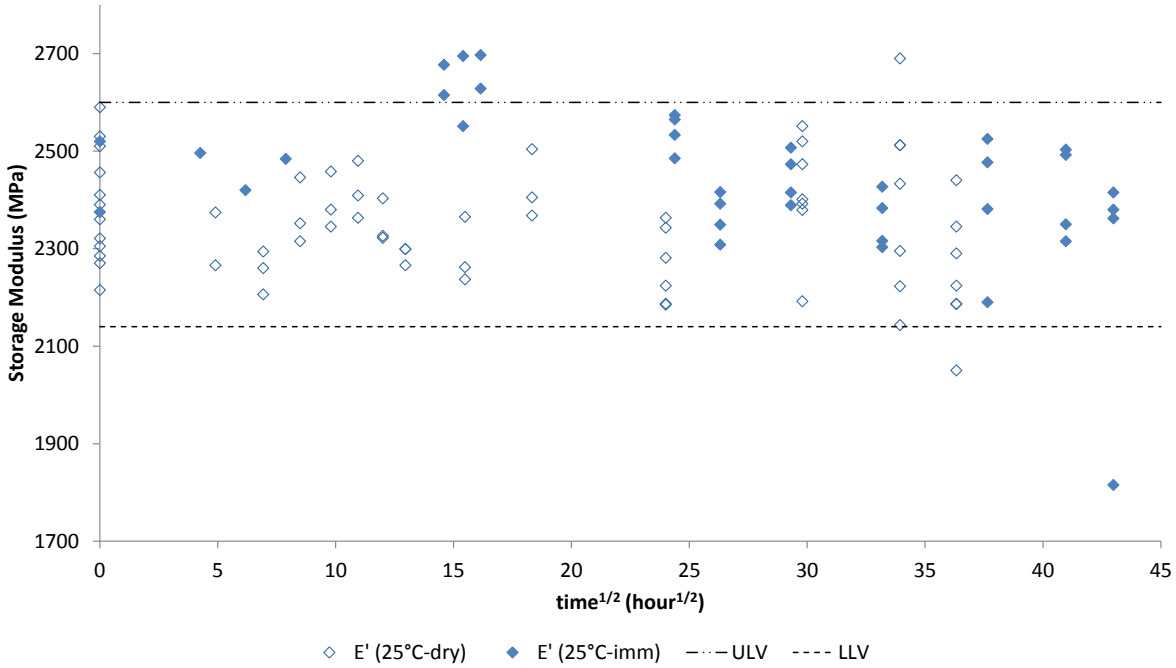

Figure 4.11. Storage modulus dry-immersed conditions at 25 °C.

4.3 Viscoelastic study as function of temperature

In this section, the DMA responses with temperature ramp are presented for the samples exposed to the conditions listed in Table 4.4.

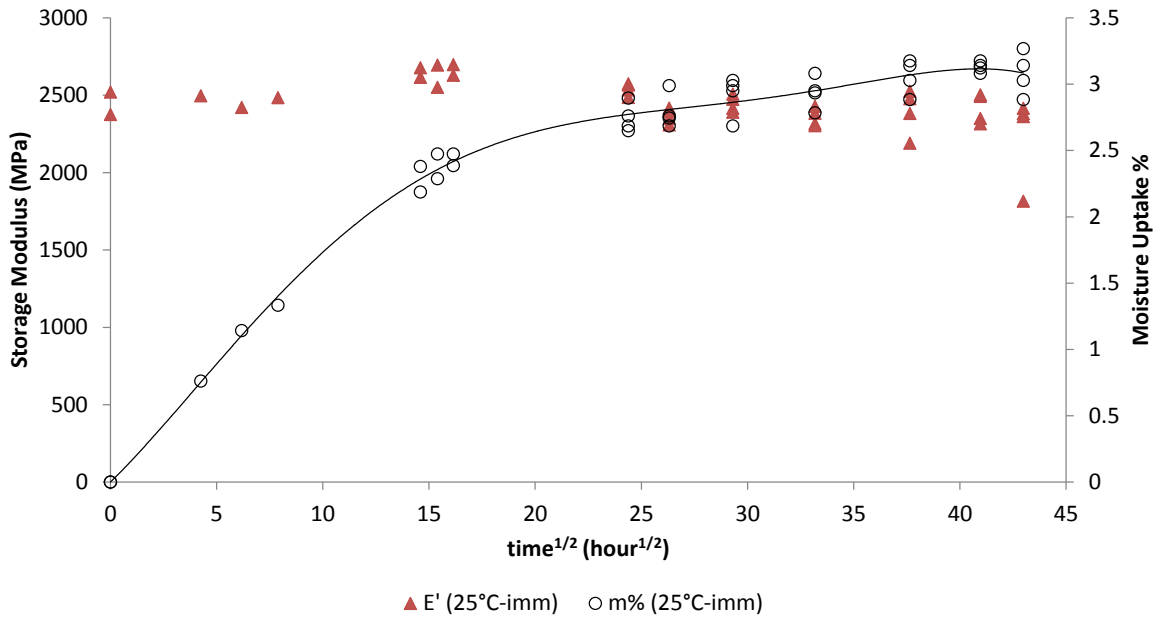

Figure 4.12. Storage modulus and moisture uptake as function of time for immersed condition.

4.3.1 Dry specimens and immersion

The physical aging process occurs because the polymers are not in thermodynamic equilibrium in their glassy state and there is a constant time-dependent effect that reduces the free-volume [16]. Thermosetting resins do not normally exhibit significant thermal aging effects when subjected to temperatures well below the T_g [36]; however, there is still some concern about certain intrinsic properties changing such as the molecular configuration and the free volume, which could create appreciable changes in physical and mechanical properties including viscoelastic properties when exposed for extended time periods. It is, thus, important to examine the component of the dynamic modulus and T_g.

When comparing the storage modulus response as a function of temperature amongst the dry specimens in Figure 4.13, a noticeable trait is the influence of aging temperature between 65 °C and 105 °C. Higher aging temperatures increased the storage modulus within this temperature range: in this case, samples exposed to 50 °C show a higher storage modulus than the ones exposed to 35 °C and 25 °C as a result of chain stiffening [47]; however, as the temperature approaches the T_g the plots converge to a single curve before dropping rapidly.

Table 4.4. Exposure time at time of T_g testing.

Temperature (°C)	Humidity (%)	Exposure time (days)	Approximate Exposure time (hours)
25	0	100	
35	0	100	**2400**
50	0	100	
35	50	80	
35	93	80	**2000**
50	50	80	
50	93	80	
25	imm	120	**2880**

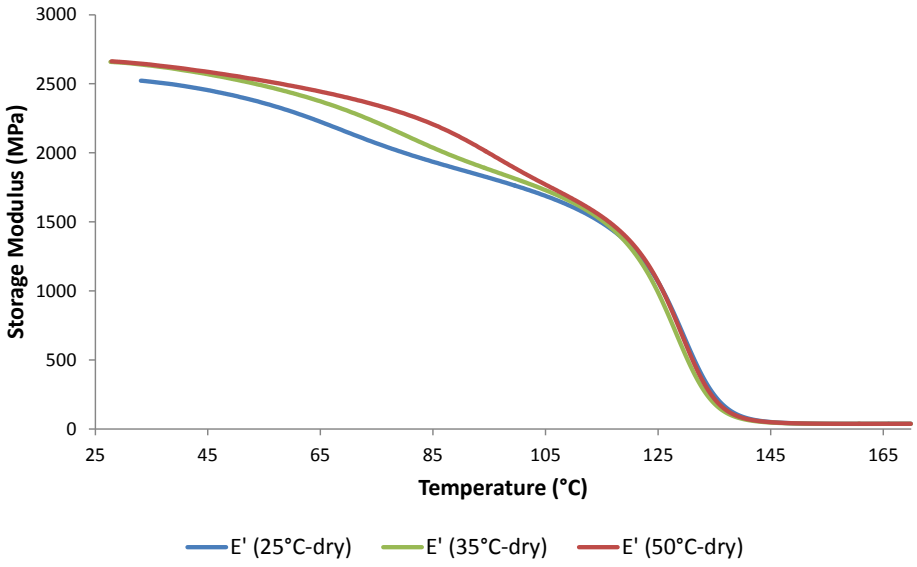

Figure 4.13. Storage modulus as a function of temperature. Dry condition exposure for 100 days.

When the loss modulus response is observed (Figure 4.14), there is a distinctive difference in the curves before the onset of T_g. Beginning at 65 °C, the loss modulus tends to decrease slightly with temperature, i.e., 50 °C observe lower loss modulus that 35 °C and 25 °C. This observation can also be attributed to chain stiffening observed in the storage modulus plots in the same region. However, as samples reach the T_g no difference is observed amongst them. This result is consistent with what is reported in the literature [50] in relation to the mechanisms of physical aging. Additionally, in our tests no

measurable vertical shifts in the T_g peaks are observed either for the relatively low aging temperatures used. This result is particularly relevant in this work since it serves as a reference for comparing with hygrothermal conditions.

Finally, the *tan* δ curves (Figure 4.15) for all samples subjected to the dry conditions are the same. All the curves overlap almost perfectly.

As expected, results for the room temperature immersed samples are very different from the dry ones (Figure 4.16). Namely, storage modulus was significantly reduced because of plasticization prior to the onset of T_g.

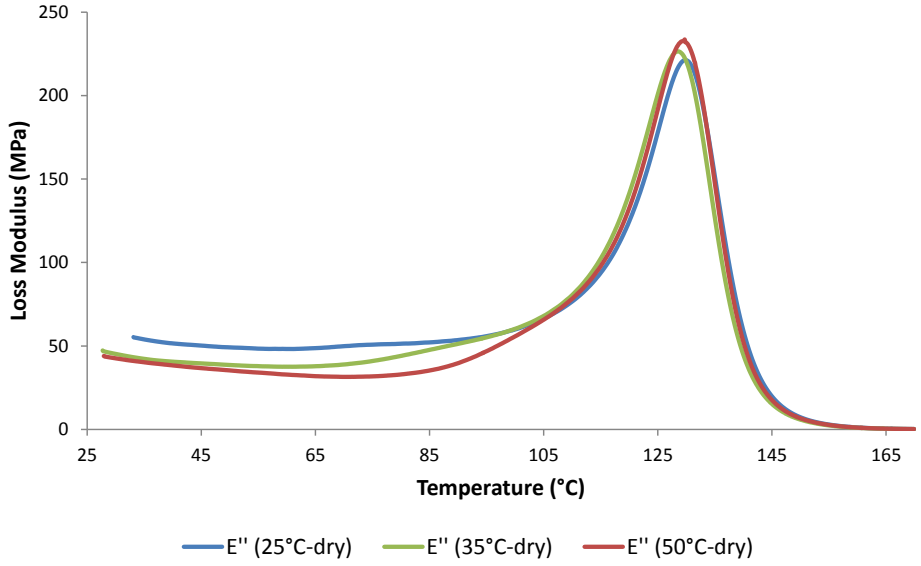

Figure 4.14. Loss modulus as a function of temperature. Dry conditions at 100 days.

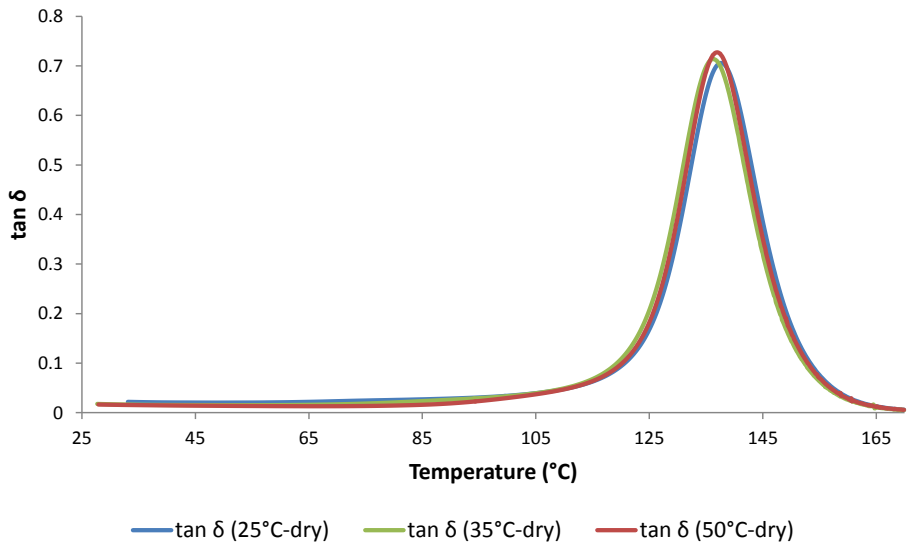

Figure 4.15. Tan δ as a function of temperature. Dry conditions at 100 days.

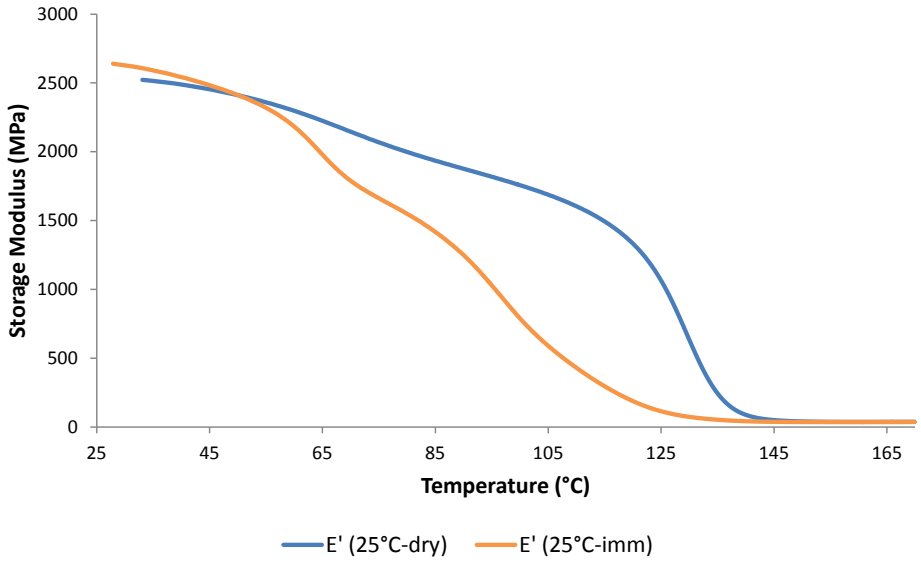

Figure 4.16. Storage modulus as a function of temperature. Dry conditions at 100 days and 25°C-imm at 120 days.

The results for loss modulus and *tan δ* (Figure 4.17 and Figure 4.18) indicate that water uptake clearly affects the T_g and the damping factor by shifting the curves down, as well as to lower temperatures while broadening the area under the curve. This implies that the presence of water not only acts as a plasticizer

but at the same time, the molecular relaxation behaviour shifts to lower temperatures where shorter and different chain lengths are able to move [51]. The "shoulders" present on both side of the T_g could be attributed to the water drying out of the samples unevenly as the test progresses [6, 52].

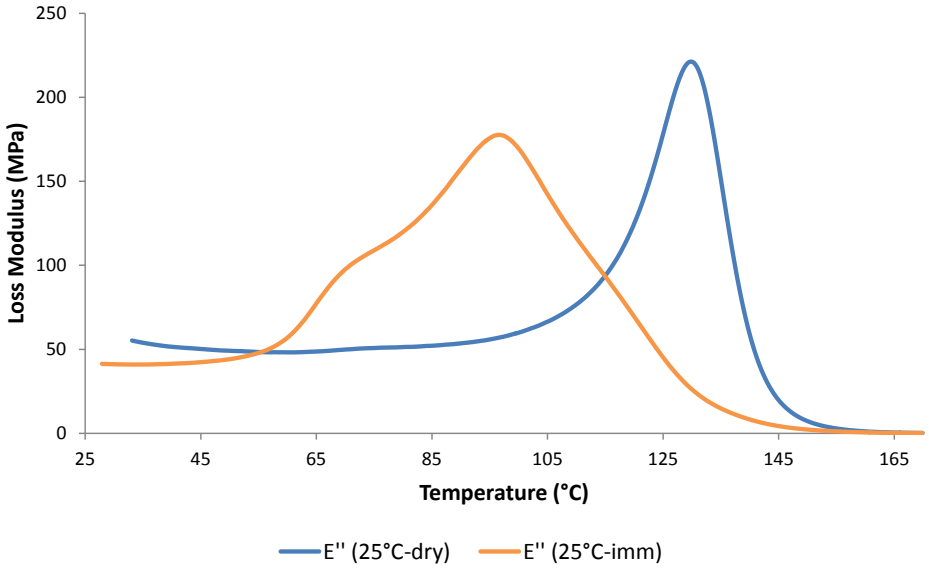

Figure 4.17. Loss modulus as a function of temperature. Dry conditions at 100 days and 25°C-imm at 120 days.

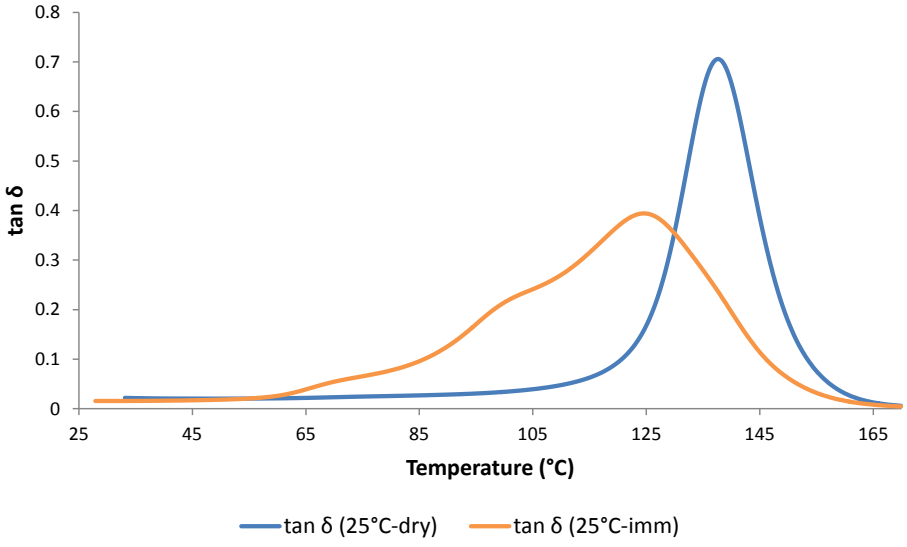

Figure 4.18. Tan δ as a function of temperature. Dry conditions at 100 days and 25°C-imm at 120 days.

It has been recognized in the literature that the glass transition value, T_g, determined from the loss modulus and the *tan δ* peaks are different. This has been attributed to the different levels of molecular motion that the DMA detects in each case. As mentioned by Menczel and Prime [20], the maximum loss modulus should be regarded as the most practical measurement rather than the maximum *tan δ* since it shows the initiation of segmental motions associated with the softening point, while the maximum *tan δ* indicates the temperature well into the softening point. In this sense, at the maximum loss modulus peak, the shorter segmental chains start to move, but it is not until the material reaches the *tan δ* temperature that the movement propagates into a cooperative motion among the longer chains. Corresponding values for T_g *(E'')* and T_g *(tan δ)* are shown in Table 4.5.

4.3.2 Effects of Temperature and RH interactions

The influence of varying relative humidities (at constant temperature) on the storage modulus is discussed in this section.

In Figure 4.19 and Figure 4.20, the storage modulus response was different for each hygrothermal exposure, noting that an increase in relative humidity tends to reduce the storage modulus with more substantive reductions starting at around 85 °C – consistent with literature reports [24].

In Figure 4.21 a comparison of all the storage modulus curves is shown for 100 days exposure for dry conditions and 120 days of exposure for 25°C-imm.

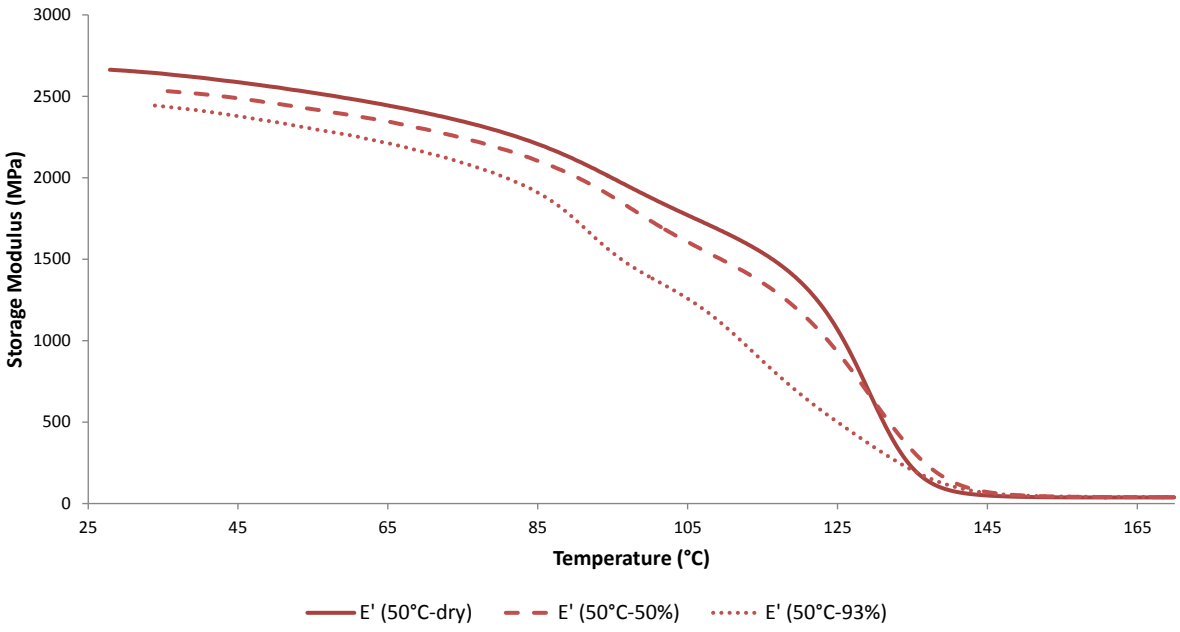

Figure 4.19. RH effect on storage modulus at 50 °C. Dry conditions at 100 days and hygrothermal conditions at 80 days.

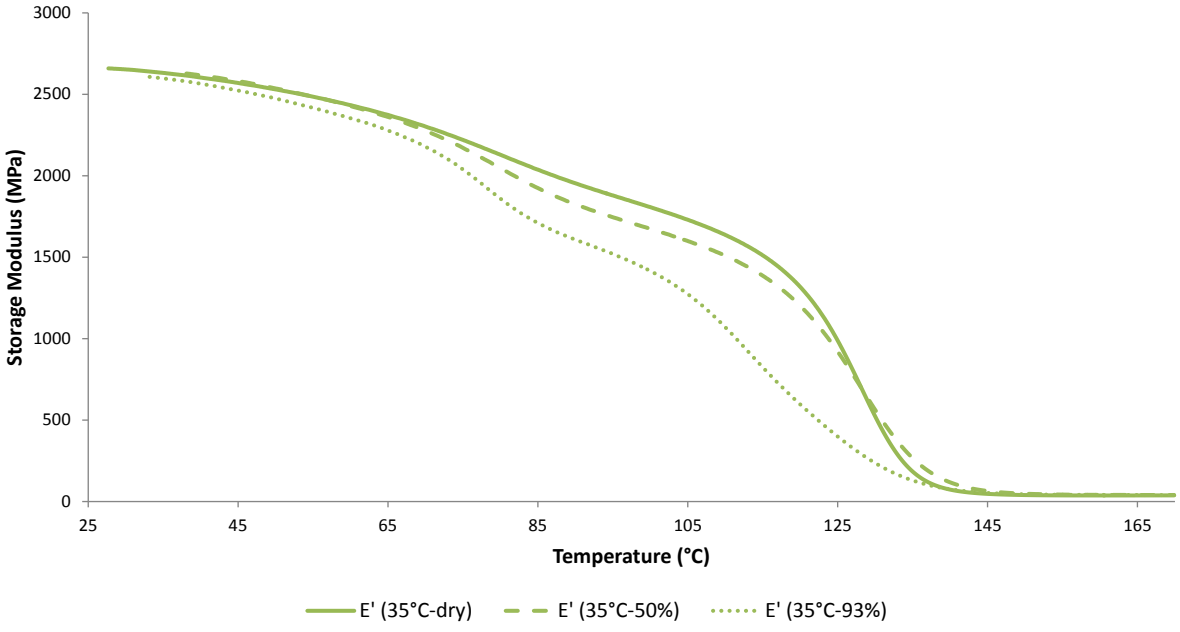

Figure 4.20. RH effect on storage modulus at 35 °C. Dry conditions at 100 days and hygrothermal conditions at 80 days

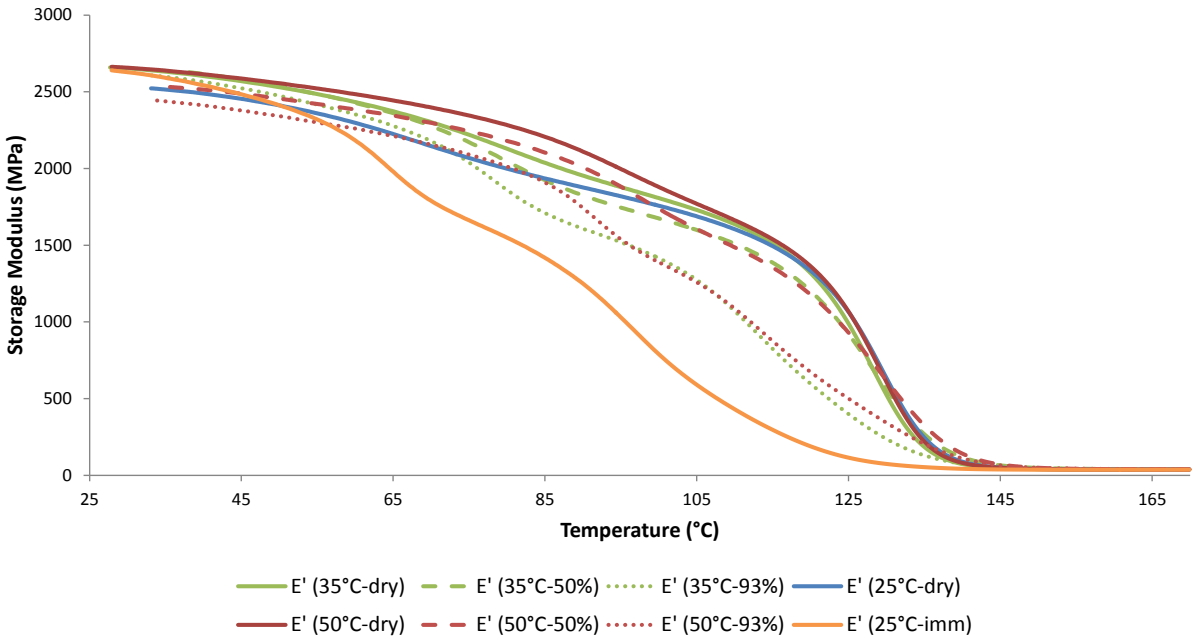

Figure 4.21. Storage modulus for all conditions. Dry conditions at 100 days, hygrothermal conditions at 80 days and 25°C-immersed at 120 days.

4.3.3 T_g comparison

The T_g results as obtained from the temperature readings at the peak of the loss modulus and at the peak of the *tan* δ in Figure 4.26 and Figure 4.27 are summarized in Table 4.5 (average of three values).

When comparing the T_g values, temperature alone (i.e., dry conditions) has a negligible effect on the value, for the relatively low range of temperatures studied. This result agrees with expected epoxy behaviour when it is not subjected to moisture exposure [36]. However, when moisture is added, significant effects can be observed on the T_g. For instance, when analyzing the effects of temperature and RH on mass uptake, the most influential parameter appears to be the RH (Appendix C). The above results show that relative humidity plays a predominant role in affecting the behaviour of T_g *(E'')*, and the damping peaks (i.e., loss modulus peak and *tan* δ peak). A plausible explanation is that the value of T_g *(E'')* is very sensitive to small molecular motions that generally occur at lower temperatures. As noted by Zhou et al. [53], T_g is not necessarily only correlated to the water uptake but to the complete hygrothermal history of the material. In the case of T_g (*tan* δ), our data reveals that there is an interaction effect only when relative humidity is coupled with temperature.

Table 4.5. T_g measurements by DMA.

Condition	T_g E'' (°C)	SD (°C)	T_g tan δ (°C)	SD (°C)	E'' peak (MPa)	SD (MPa)	tan δ peak (-)	SD (-)	M_∞ %
25°C-dry	130.06	1.24	137.67	1.67	223.67	20.14	0.730	0.026	--
35°C-dry	128.67	1.45	136.23	1.50	230.97	5.75	0.730	0.015	--
50°C-dry	129.73	1.70	137.00	1.47	237.53	3.60	0.741	0.008	--
25°C-Imm	95.23	1.82	123.07	2.59	179.97	9.01	0.397	0.006	3.20
35°C-50%	128.56	1.82	139.03	2.11	219.57	9.17	0.675	0.017	1.33
35°C-93%	113.06	0.46	135.83	1.30	173.27	6.71	0.489	0.025	2.93
50°C-50%	129.53	1.90	140.70	1.51	195.03	24.6	0.662	0.019	1.30
50°C-93%	113.70	0.53	140.37	1.30	158.70	6.06	0.517	0.010	3.30

In order to quickly compare the relative humidity conditions, boxplot diagrams are drawn in Figure 4.22 to Figure 4.25. A boxplot is a visual representation that highlights the maximum and minimum, represented by "whiskers"; the likely range of variation, represented by the contour of the box (first to third quartile) and the median. Measurements located 1.5 times outside the quartiles are considered suspect outliers while measurements further than 3 times are definite outliers.

These diagrams indicate on Figure 4.22 that a humidity increase from the dry condition up to 50% RH does not affect the T_g *(E'')*, whereas there is significant difference when the RH is increased to 93%. An important distinction on the T_g *(tan δ)* (Figure 4.23) is seen when increasing RH to 50% from the dry condition, both temperatures (35 °C and 50 °C) appear to generate a small increase in T_g (*tan δ)* but when humidity rises even further, only the samples exposed to 35 °C show a decreased T_g (*tan δ)* value. The samples exposed to 50 °C did not experience change when the humidity was raised from 50% RH to 93%. This suggests that humidity impacts behaviour at 35 °C but not at 50 °C in the same way: the discussions about T_g (*tan δ)* being less sensitive to smaller variations of temperatures is demonstrated again. Overall for all the parameters, except T_g *(tan δ)*, it is clear that material properties are reduced as conditions become more severe.

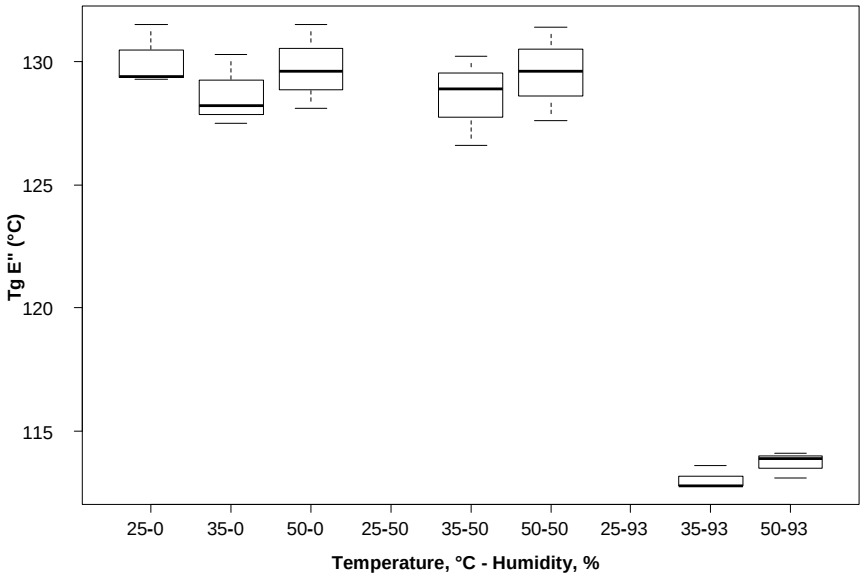

Figure 4.22. Boxplot T_g (E'') as function of T and RH. Dry: 100 days. Hygrothermal: 80 days.

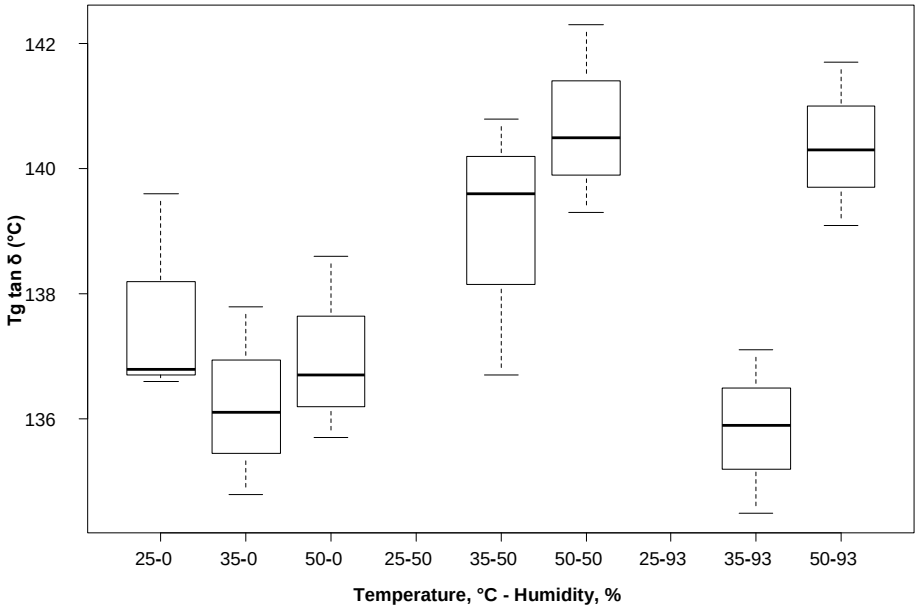

Figure 4.23. Boxplot T_g *(tan δ)* as function of T and RH. Dry: 100 days. Hygrothermal: 80 days.

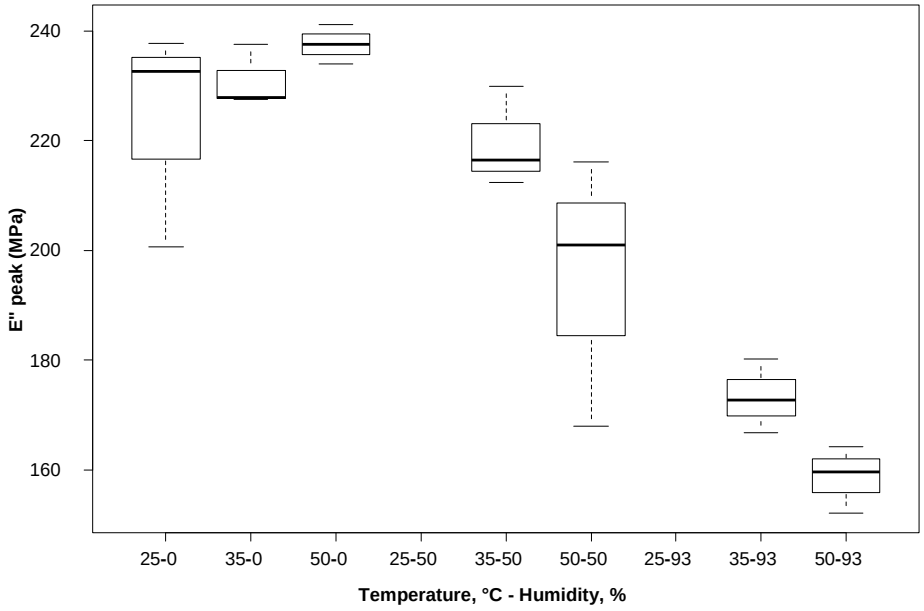

Figure 4.24. Boxplot E'' max peak as function of T and RH. Dry: 100 days. Hygrothermal: 80 days.

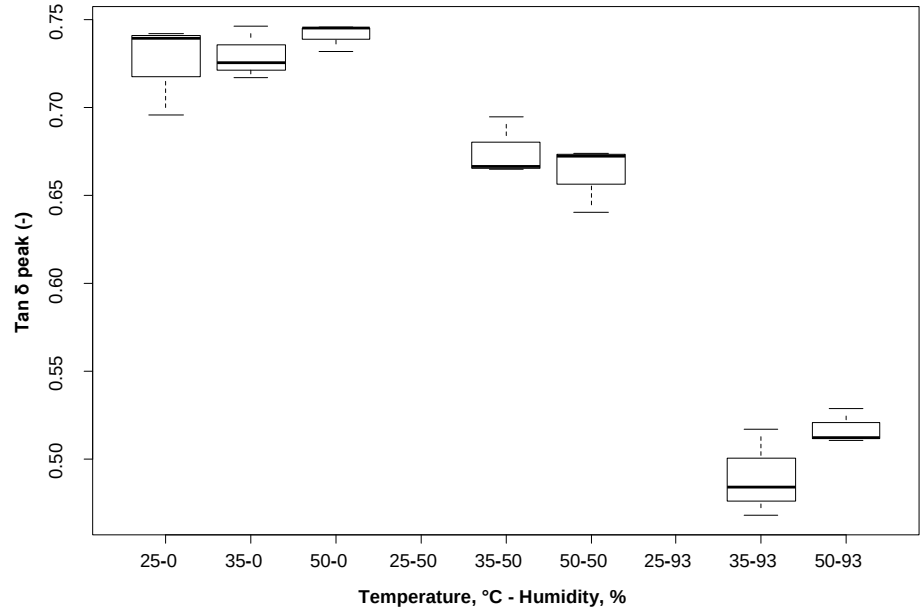

Figure 4.25. Boxplot *tan δ* max peak as function of T and RH. Dry: 100 days. Hygrothermal: 80 days.

Finally, it is noted that the water content of the material in itself is not a direct determinant of the T_g value, as the overall hygrothermal history of the epoxy will impact the value. This may be related to the complexity of the diffusion mechanisms that can occur during water absorption in the DGEBA/TETA system.

Figure 4.26 shows that consistent with behaviour of highly plasticized polymer, the T_g value for immersed sample is the lowest, followed by the 93% RH and 50% RH, respectively. Dry condition effects on T_g are minimal. Plasticized epoxy tends to generate broader peaks than dry epoxy and the height of the peaks decreases with increasing exposure temperature. For the immersed epoxy, the peak is both broad and high which translates to higher damping capacity over a wider range of temperatures.

When comparing Figure 4.26 and Figure 4.27, it would appear that the loss modulus is better able to separate the effects of moisture absorption than the *tan* δ curves. The trends are similar but the T_g differences are less discernible. This suggests that loss modulus is a more sensitive parameter for characterizing changes in lower energy localized molecular motions. However, another important observation on this plot can be summarized as follows:

Papanicolaou et al. [9] while analyzing related epoxy-amine composition noted that T_g (*tan* δ) tended to increase when immersed at 60 °C and 80 °C. In our case a slight increase was observed only when exposed to relative humidity conditions and not during immersed conditions. Thus, it can be inferred that temperature when coupled with humidity has different effects depending on the intensity of the conditions. For example, at 35°C-50% the curves tended to shift towards higher T_g but when increasing RH to 93% it returned towards lower T_g. A similar behaviour is observed in 50°C-50% and 50°C-93%. This implies that a small increase in temperature is sufficient to counter the apparent decreasing effects of water on the T_g. The extreme case (immersed and lower temperatures) shifts the T_g towards lower values. Among the literature, Zhou and Lucas note that Type II hydrogen bondings are formed due to the interaction of water and epoxy and only the T_g (*tan* δ) seems to discern this behaviour [53].

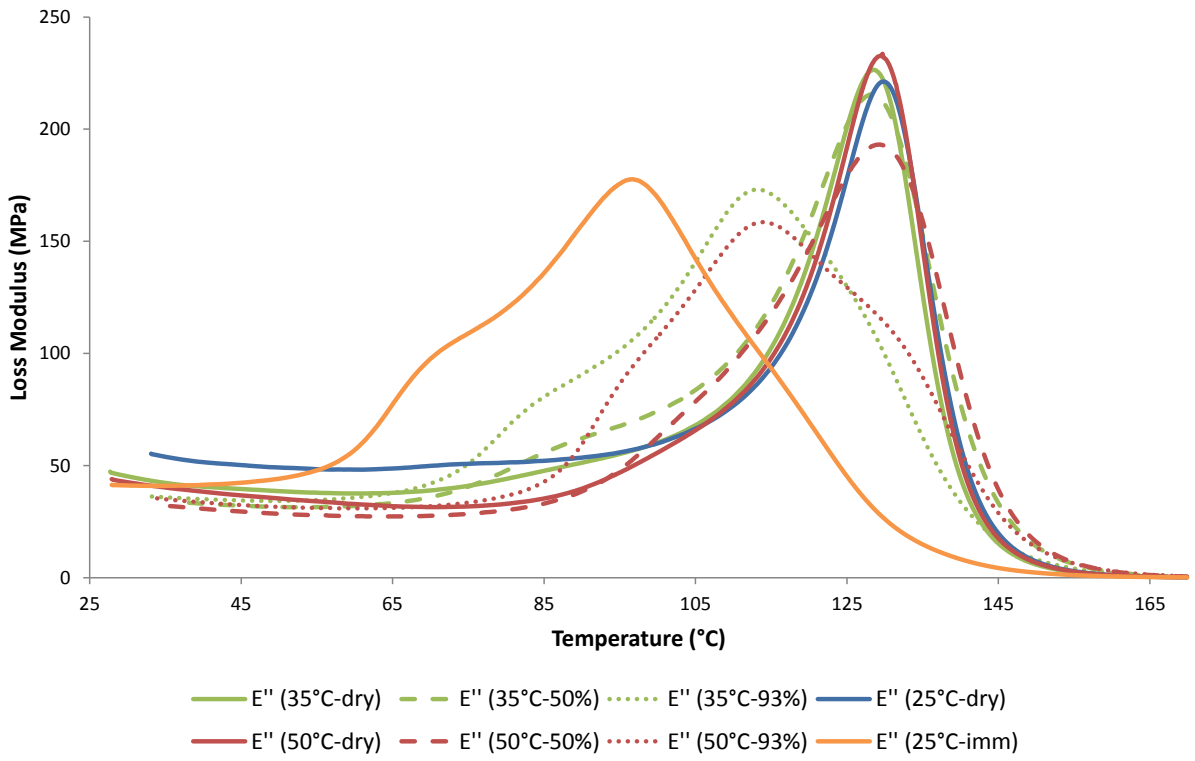

Figure 4.26. Loss modulus as function of T. Dry: 100 days. Hygrothermal: 80 days. 25°C-imm: 120 days.

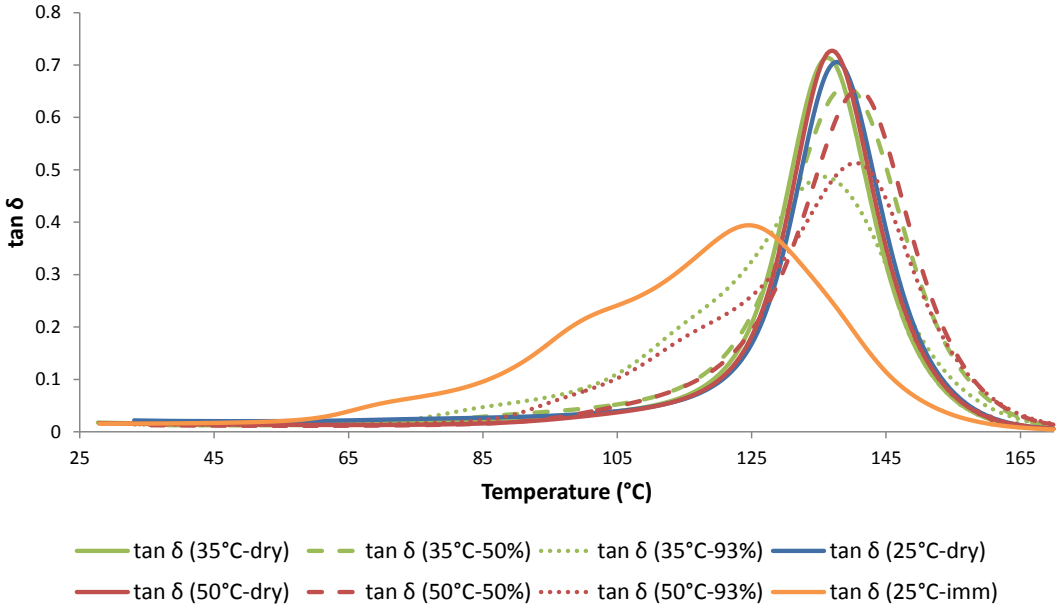

Figure 4.27. Tan δ as function of T. Dry: 100 days. Hygrothermal: 80 days. 25°C-imm: 120 days.

Chapter 5
Conclusions and Recommendations

5.1 Conclusions

The current study on the effects of hygrothermal aging on the dynamic mechanical response of DGEBA/TETA has led to the following conclusions:

1. Based on gravimetric measurements, it was found that water uptake under the five hygrothermal conditions tested occurred through non-Fickian diffusion. This mechanism is characterized by predominant influence from the relaxation mode. Generally, diffusion coefficients could be obtained from the linear portion of the uptake curve (< 60%) for hygrothermal conditions but not for the completely immersed condition. It can be inferred that in samples exposed to higher relative humidity (including immersed) condition, temperature is an important factor in determining if behaviour is Fickian or non-Fickian. At ambient temperatures, the Fickian diffusion model cannot be reliably used to estimate the diffusion coefficient.

2. The dynamic mechanical properties of epoxy material are highly dependent on the hygrothermal aging conditions, such as temperature, relative humidity and exposure time. At ambient testing of storage modulus, it was found that dry aging conditions had a detrimental effect on the modulus as exposure time increased. This effect, however, was attenuated when coupled with relative humidity conditions, resulting in no net change. This behaviour is most likely associated with reported intrinsic submolecular mechanisms occurring in the material such as the hydrogen bondings occurring in the polymer (Type II specifically).

3. When DMA testing is performed after 80 days and by temperature ramping, there are marked differences in curves at temperatures below the onset of glass transition temperature. Dry aging conditions increased storage modulus while the presence of relative humidity had the reverse effect. This suggests that temperature ramp-up test method is better able for detecting differences in behaviour due to physical aging and plasticization.

4. At temperatures above T_g, the storage modulus, loss modulus and *tan* δ properties are markedly influenced by the exposure temperature and relative humidities. The glass transition, T_g , and damping

factor are greatly affected by humidity, a parameter found to be more influential than temperature in this study. This could be attributed to plasticization and the hygrothermal history of the material.

5. Two types of T_g were analyzed, one obtained from the loss modulus peak and the other obtained from the *tan* δ peak. These measurements, although similar in name, represent different molecular mechanisms involved and in the case of the T_g determined by loss modulus method, the relative humidity was found to have detrimental effects on the epoxy. However, the T_g determined by *tan* δ should not be ignored since it likely represents the cooperative molecular motions involving hydrogen bonding.

5.2 Recommendations

To further expand this topic of study on DGEBA/TETA, it is recommended to:

1. Conduct a test to estimate the coefficient of thermal expansion (CTE or α) in this material for the current conditions. This test is especially important when considering adding fillers to the base material because different CTE between materials are the prime cause of internal stresses. It is expected that different humidity conditions will alter the CTE. Likewise, it is recommended to calculate the coefficient of hygroscopic swelling (CHS or β). This is another useful parameter to consider when manufacturing composites, since it allows quantifying internal stresses associated with water uptake. A combined TMA/TGA procedure to aid their determination is proposed by other authors [54].

2. Expose samples to cyclic temperature-humidity testing to determine and compare possible additional effects. Some researchers have studied this in other materials but to the knowledge of this author, nothing has been conducted in DGEBA/TETA epoxies. Cyclic temperature-humidity testing will allow the determination of the intrinsic relationship between chemical potential, mass flux and temperature variation on the material, which is the foundational procedure for novel types of simulation.

3. Study the applicability of non-Fickian models on the epoxy-amine system such as the Langmuir model. This will allow an accurate prediction of the final equilibrium mass uptake.

4. Study DMA properties using dried samples (after exposure) to study the effects of removed water on the T_g behaviour and elastic modulus of the epoxy.

Bibliography

[1] Y. C. Lin and X. Chen, "Moisture sorption-desorption-resorption characteristics and its effect on the mechanical behavior of the epoxy system," *Polymer*, vol. 46, pp. 11994-12003, 2005.

[2] J. P. Pascault, H. Sautereau, J. Verdu and R. Williams, *Thermosetting Polymers.* 2002.

[3] J. R. M. d'Almeida, G. W. d. Menezes and S. N. Monteiro, "Ageing of the DGEBA/TETA epoxy system with off-stoichiometric compositions," *Materials Research*, vol. 6, pp. 415-420, 2003.

[4] M. H. Shirangi, X. J. Fan and B. Michel, "Mechanism of moisture diffusion, hygroscopic swelling and adhesion degradation in epoxy molding compounds," in *41st Annual International Symposium on Microelectronics, IMAPS 2008, November 2, 2008 - November 6*, 2008, pp. 1082-1089.

[5] S. Z. Cheng, *Handbook of Thermal Analysis and Calorimetry: Applications to Polymers and Plastics.* Elsevier, 2002.

[6] K. I. Ivanova, R. A. Pethrick and S. Affrossman, "Hygrothermal aging of rubber-modified and mineral-filled dicyandiamide-cured DGEBA epoxy resin. II. Dynamic mechanical thermal analysis," *J Appl Polym Sci*, vol. 82, pp. 3477-3485, 2001.

[7] J. A. Hough, S. K. Karad and F. R. Jones, "The effect of thermal spiking on moisture absorption, mechanical and viscoelastic properties of carbon fibre reinforced epoxy laminates," *Composites Sci. Technol.*, vol. 65, pp. 1299-1305, 2005.

[8] L. Núñez, M. Villanueva, F. Fraga and M. Nunez, "Influence of water absorption on the mechanical properties of a DGEBA (n= 0)/1, 2 DCH epoxy system," *J Appl Polym Sci*, vol. 74, pp. 353-358, 1999.

[9] G. Papanicolaou, T. V. Kosmidou, A. Vatalis and C. Delides, "Water absorption mechanism and some anomalous effects on the mechanical and viscoelastic behavior of an epoxy system," *J Appl Polym Sci*, vol. 99, pp. 1328-1339, 2006.

[10] P. Theocaris, E. Kontou and G. Papanicolaou, "The effect of moisture absorption on the thermomechanical properties of particulates," *Colloid Polym. Sci.*, vol. 261, pp. 394-403, 1983.

[11] A. Apicella, L. Nicolais, G. Astarita and E. Drioli, "Effect of thermal history on water sorption, elastic properties and the glass transition of epoxy resins," *Polymer*, vol. 20, pp. 1143-1148, 1979.

[12] P. Nogueira, C. Ramirez, A. Torres, M. J. Abad, J. Cano, J. Lopez, I. Lopez-Bueno and L. Barral, "Effect of water sorption on the structure and mechanical properties of an epoxy resin system," *J Appl Polym Sci*, vol. 80, pp. 71-80, 2001.

[13] C. Shen and G. S. Springer, "Moisture absorption and desorption of composite materials," *J. Composite Mater.*, vol. 10, pp. 2-20, 1976.

[14] S. Roy, W. Xu, S. Park and K. Liechti, "Anomalous moisture diffusion in viscoelastic polymers: modeling and testing," *Journal of Applied Mechanics*, vol. 67, pp. 391-396, 2000.

[15] K. P. Menard, *Dynamic Mechanical Analysis: A Practical Introduction.* CRC press, 2008.

[16] Y. J. Weitsman, *Fluid Effects in Polymers and Polymeric Composites.* Springer Science & Business Media, 2011.

[17] H. Ardebili, E. H. Wong and M. Pecht, "Hygroscopic swelling and sorption characteristics of epoxy molding compounds used in electronic packaging," *Components and Packaging Technologies, IEEE Transactions On*, vol. 26, pp. 206-214, 2003.

[18] J. Zhou and J. P. Lucas, "Hygrothermal effects of epoxy resin. Part I: the nature of water in epoxy," *Polymer*, vol. 40, pp. 5505-5512, 1999.

[19] J. Mark et al., *Physical Properties of Polymers.* Cambridge University Press, 2004.

[20] J. D. Menczel and R. B. Prime, *Thermal Analysis of Polymers, Fundamentals and Applications.* John Wiley & Sons, 2009.

[21] J. D. Ferry, *Viscoelastic Properties of Polymers.* John Wiley & Sons, 1980.

[22] TA Instruments, *DMA Dynamic Mechanical Analyzer Q Series Getting Started Guide*. New Castle, DE: 2007.

[23] G. LaPlante and P. Lee-Sullivan, "Moisture effects on FM300 structural film adhesive: Stress relaxation, fracture toughness, and dynamic mechanical analysis," *J Appl Polym Sci,* vol. 95, pp. 1285-1294, 2005.

[24] T. C. Clancy, S. J. V. Frankland, J. A. Hinkley and T. S. Gates, "Molecular modeling for calculation of mechanical properties of epoxies with moisture ingress," *Polymer,* vol. 50, pp. 2736-2742, /6/5/, 2009.

[25] T. Ferguson and J. Qu, "Elastic modulus variation due to moisture absorption and permanent changes upon redrying in epoxy based underfill," *IEEE Transactions on Components and Packaging Technologies,* vol. 29, pp. 105-111, 2006.

[26] W. Loh, A. Crocombe, M. Abdel Wahab and I. Ashcroft, "Modelling anomalous moisture uptake, swelling and thermal characteristics of a rubber toughened epoxy adhesive," *Int J Adhes Adhes,* vol. 25, pp. 1-12, 2005.

[27] Dow Chemical Company, "D.E.R.™ Liquid Epoxy Resin," Form No. 296-01408-0109X-TD, 2009.

[28] D. Ratna, *Handbook of Thermoset Resins.* ISmithers, 2009.

[29] Air Products, "Epoxy curing agents and modifiers: Ancamine TETA Curing Agent," 25-9715.8, May 2007.

[30] Dow Chemical Company, "Triethylenetetramine (TETA)," Form No. 108-01353-1001 AMS, 2001.

[31] A. Handbook, "Volume 21: Composites," *American Society of Metals, International Handbook Committee,* 2001.

[32] *Standard Test Method for Tensile Properties of Thin Plastic Sheeting,* ASTM D888-12, 2012.

[33] A. D. Mazzeo, M. E. Lustrino and D. E. Hardt, "Bubble removal in centrifugal casting: Combined effects of buoyancy and diffusion," *Polym. Eng. Sci.*, vol. 52, pp. 80-90, 2012.

[34] Eppendorf AG, *Centrifuge 5430 / 5430 R Operating Manual.* Hamburg, Germany: 2012.

[35] *Standard Test Method for the Assignment of the Glass Transition Temperature by Modulated Temperature Differential Scanning Calorimetry,* ASTM E2602-09, 2009.

[36] G. M. Odegard and A. Bandyopadhyay, "Physical Aging of Epoxy Polymers and Their Composites," *Journal of Polymer Science Part B: Polymer Physics,* vol. 49, pp. 1695-1716, 2011.

[37] W.A. Hammond Drierite Co. Ltd, "Technical Data. How much Drierite?" Available: https://secure.drierite.com/catalog3/page17b.cfm, Accessed Oct 2014.

[38] *Environmental Testing - Part 2-78: Tests - Test Cab: Damp heat, steady state,* IEC 60068-2-78, 2012.

[39] *Standard Test Method for Water Absorption of Plastics,* ASTM D570-98, 2010.

[40] M. Haghighi-Yazdi, J. K. Y. Tang and P. Lee-Sullivan, "Moisture uptake of a polycarbonate blend exposed to hygrothermal aging," *Polym. Degrad. Stab.*, vol. 96, pp. 1858-1865, 10, 2011.

[41] S. Joannès, L. Mazé and A. R. Bunsell, "A concentration-dependent diffusion coefficient model for water sorption in composite," *Composite Structures,* vol. 108, pp. 111-118, 2014.

[42] L. Wu and S. V. Hoa, "Effects of composition of hardener on the curing and aging for an epoxy resin system," *J Appl Polym Sci,* vol. 99, pp. 580-588, 2006.

[43] C. L. Soles and A. F. Yee, "A discussion of the molecular mechanisms of moisture transport in epoxy resins," *Journal of Polymer Science Part B: Polymer Physics,* vol. 38, pp. 792-802, 2000.

[44] L. Cai and Y. Weitsman, "Non-Fickian moisture diffusion in polymeric composites," *J. Composite Mater.*, vol. 28, pp. 130-154, 1994.

[45] H. G. Carter and K. G. Kibler, "Langmuir-type model for anomalous moisture diffusion in composite resins," *J. Composite Mater.*, vol. 12, pp. 118-131, 1978.

[46] G. LaPlante, A. V. Ouriadov, P. Lee-Sullivan and B. J. Balcom, "Anomalous moisture diffusion in an epoxy adhesive detected by magnetic resonance imaging," *J Appl Polym Sci,* vol. 109, pp. 1350-1359, 2008.

[47] L. Barral, J. Cano, J. Lopez, I. Lopez-Bueno, P. Nogueira, M. Abad and C. Ramirez, "Physical aging of an epoxy/cycloaliphatic amine resin," *European Polymer Journal,* vol. 35, pp. 403-411, 1999.

[48] J. K. Lee, J. Y. Hwang and J. Gillham, "Erasure below glass-transition temperature of effect of isothermal physical aging in fully cured epoxy/amine thermosetting system," *J Appl Polym Sci,* vol. 81, pp. 396-404, 2001.

[49] A. Stimoniaris, C. Stergiou and C. Delides, "A detailed study of α-relaxation in epoxy/carbon nanoparticles composites using computational analysis," *Express Polymer Letters,* vol. 6, pp. 120-128, 2012.

[50] E. S. Kong, "Physical aging in epoxy matrices and composites," in *Epoxy Resins and Composites IV* Springer, 1986, pp. 125-171.

[51] Cambridge Polymer Group, Inc, "Glass Transition by DMA," CPGAN #035, 2014.

[52] G. Ten Brinke, F. E. Karasz and T. S. Ellis, "Depression of glass transition temperatures of polymer networks by diluents," *Macromolecules,* vol. 16, pp. 244-249, 1983.

[53] J. Zhou and J. P. Lucas, "Hygrothermal effects of epoxy resin. Part II: variations of glass transition temperature," *Polymer,* vol. 40, pp. 5513-5522, 1999.

[54] J. Zhou, T. Tee and X. Fan, "Hygroscopic swelling of polymeric materials in electronic packaging: Characterization and analysis," in *Moisture Sensitivity of Plastic Packages of IC Devices* Springer, 2010, pp. 153-179.

[55] G. B. McKenna and S. L. Simon, "The glass transition: Its measurement and underlying physics," *Handbook of Thermal Analysis and Calorimetry,* vol. 3, pp. 49-109, 2002.

Appendix A

DSC study

Differential Scanning Calorimetry (DSC) and Modulated Differential Standard Calorimetry (MDSC) studies were conducted on uncured DGEBA/TETA samples to determine the degree of cure per stage and preliminary $T_{g\infty}$ respectively. This information ensured that DMA tests results in Chapter 4 were only attributed to the environmental conditions and not variation from incomplete cure.

In order to estimate the $T_{g\infty,}$ 14.3 mg of the sample was dispensed on hermetic aluminum pans and put on a TA instruments model 2920, held for 2 hours at 135 °C, cooled down and then heated to 200 °C with modulation of ±0.80 °C every 60 seconds and underlying heat rate of 5 °C/min. The $T_{g\infty}$, measured from the step change in the reversing heat capacity [55], is approximately 120 °C (Figure A.1). The specific heat capacity of the material at 25 °C can be obtained from the same figure as well.

Since the material preparation outlined in section 3.4 involves a two-stage cure, another DSC run was performed in order to obtain the degree of cure on the first stage. The procedure for this test was as follows: 9.2 mg of liquid epoxy was dispensed in hermetic aluminum pans and tested on the same instrument. The sample was then exposed to 70 °C isothermal for 90 min, cooled and finally heated to 200 °C at a 2 °C/min heat rate to measure any possible residual.

The degree of cure (α_i) can be determined by measuring the heat of the partial reaction (ΔH_i) and the residual heat of reaction from a second heating to (ΔH_2), through the relationship $\alpha_i = \Delta H_i / (\Delta H_i + \Delta H_2)$. The heats of reaction were measured from the area under the curve of a DSC exothermic diagram. The baseline for this area measurement can be found by drawing a straight tangent line between the onset and the end of the exothermic curve [20].

Figure A.2 indicates that the bulk of the reaction (90%) occurs within the first hour of the test at 70 °C isothermal and that the final residual is eliminated between 85 °C and 130 °C; thus, the two-stage curing is adequate.

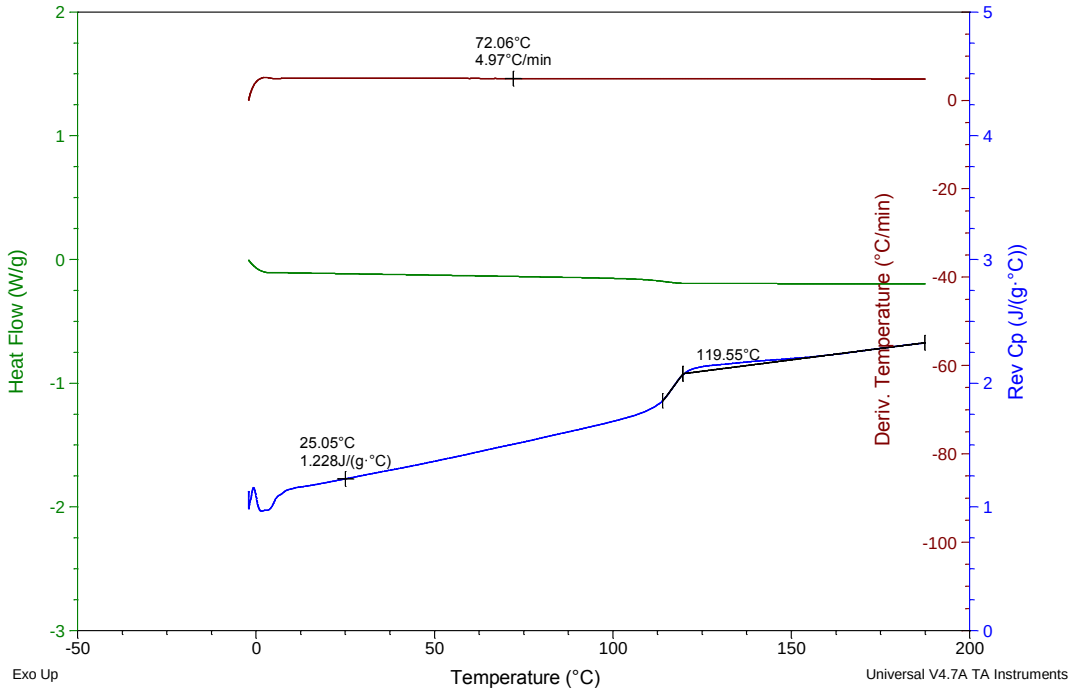

Figure A.1. MDSC Reversing C_p as function of temperature.

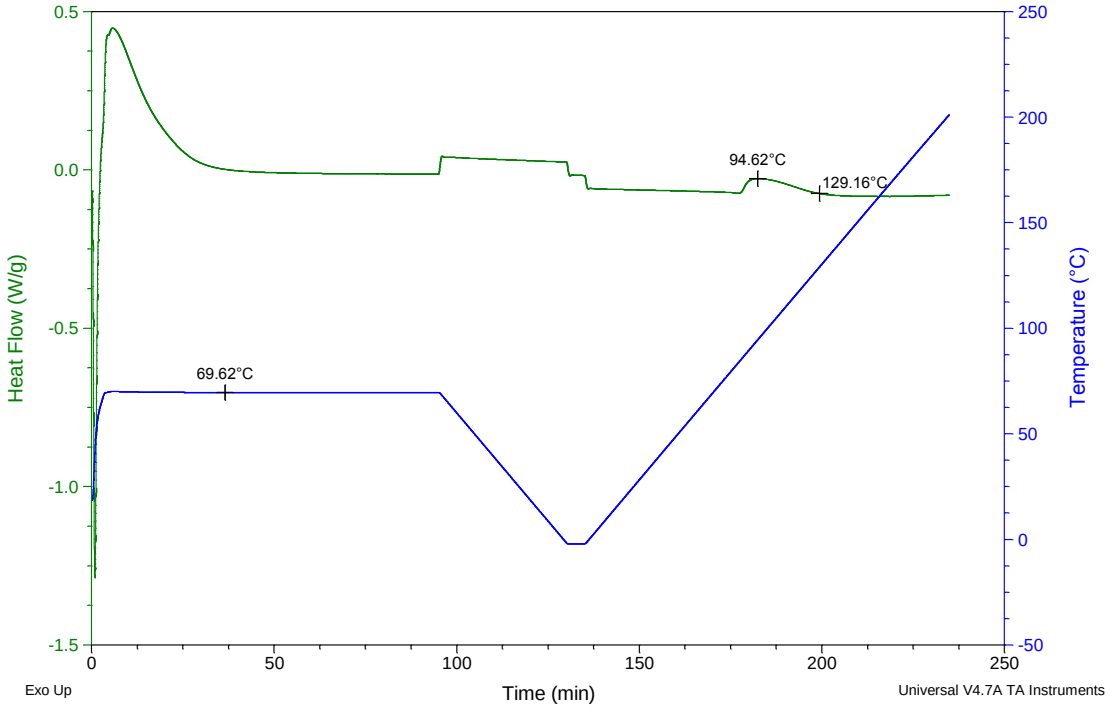

Figure A.2. DSC Heat flow and temperature as function of time.

Appendix B

Drawings

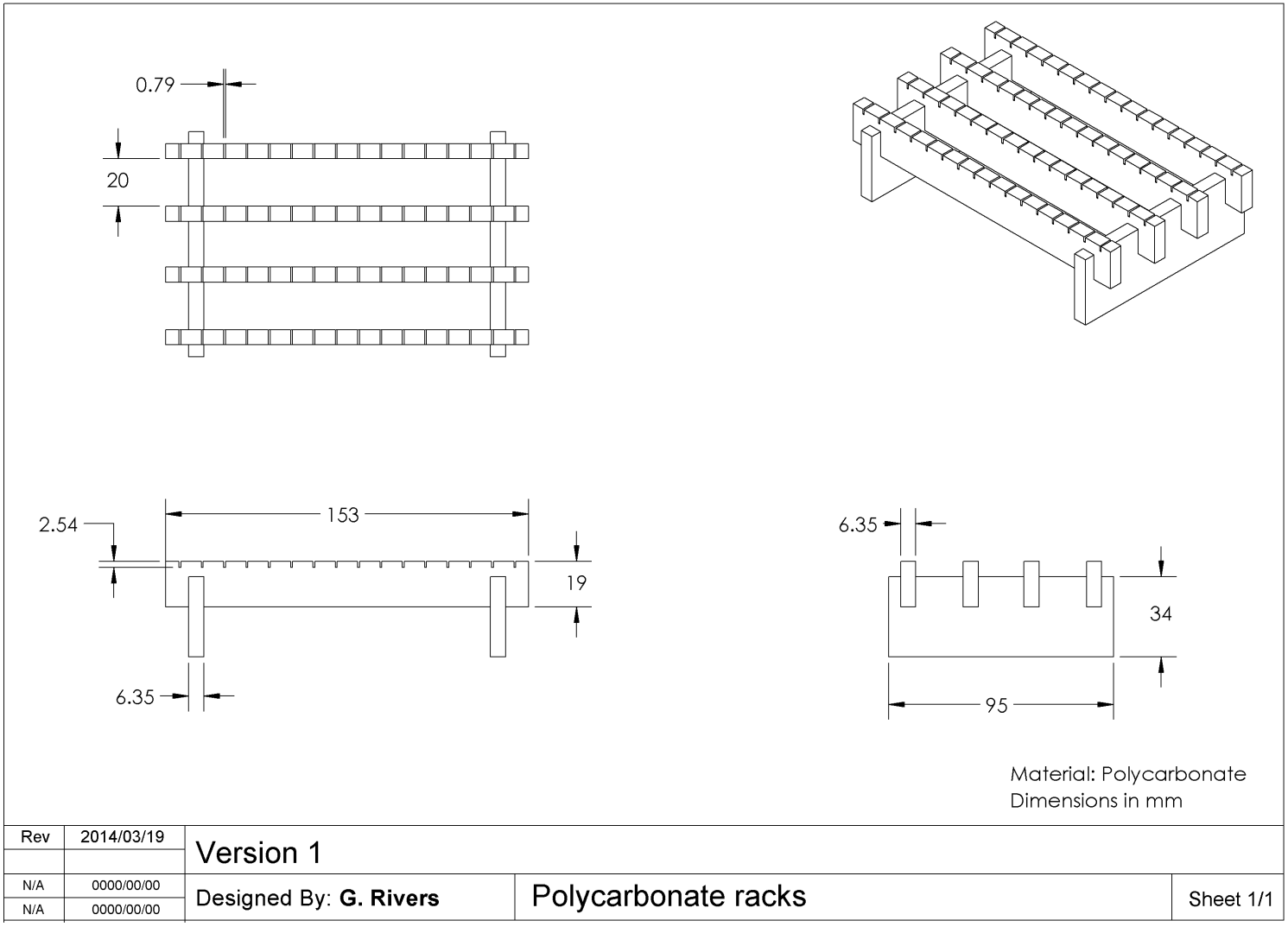

Figure B.3. Polycarbonate racks.

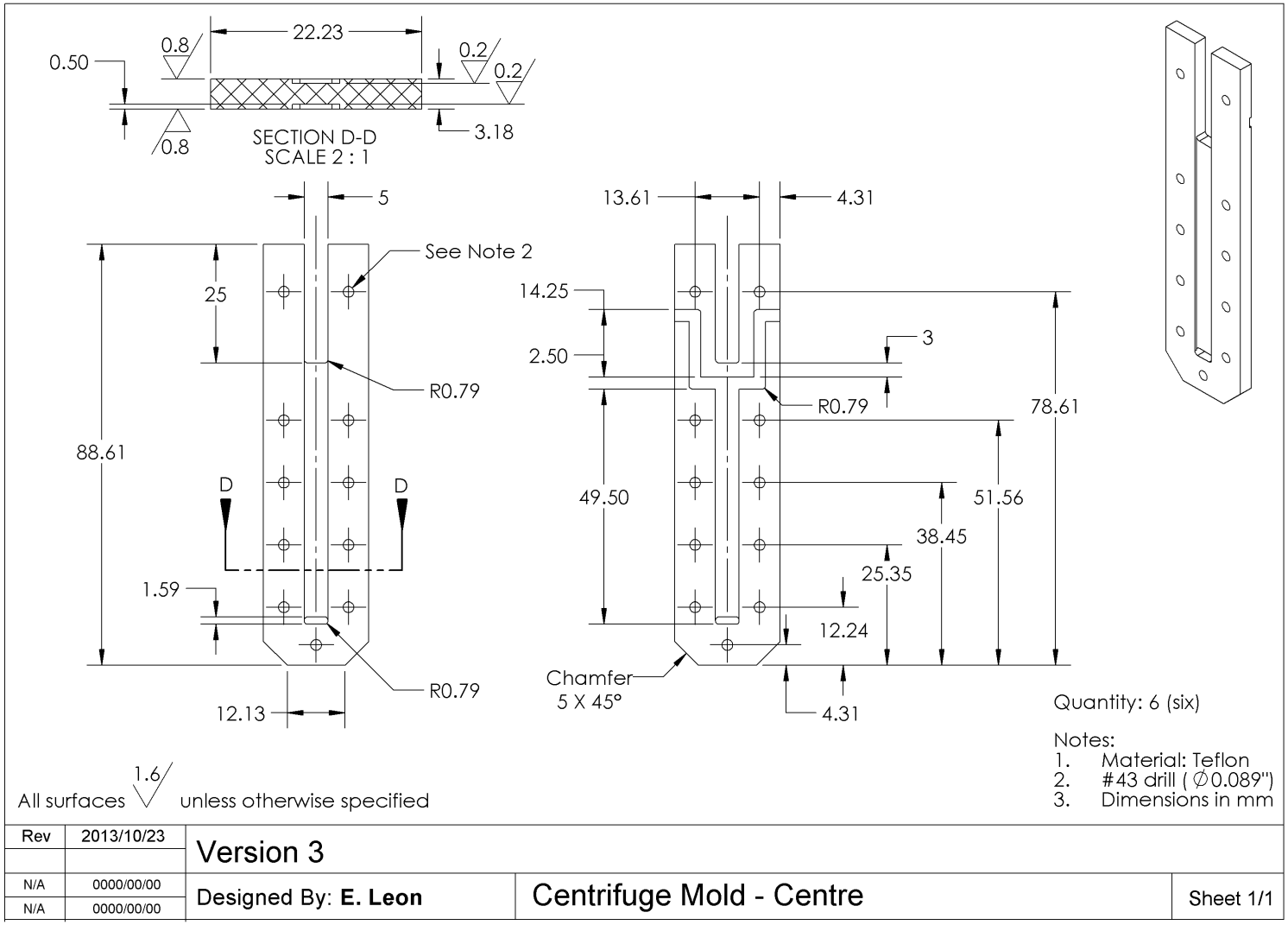

Figure B.4. Centrifuge Mold – Centre.

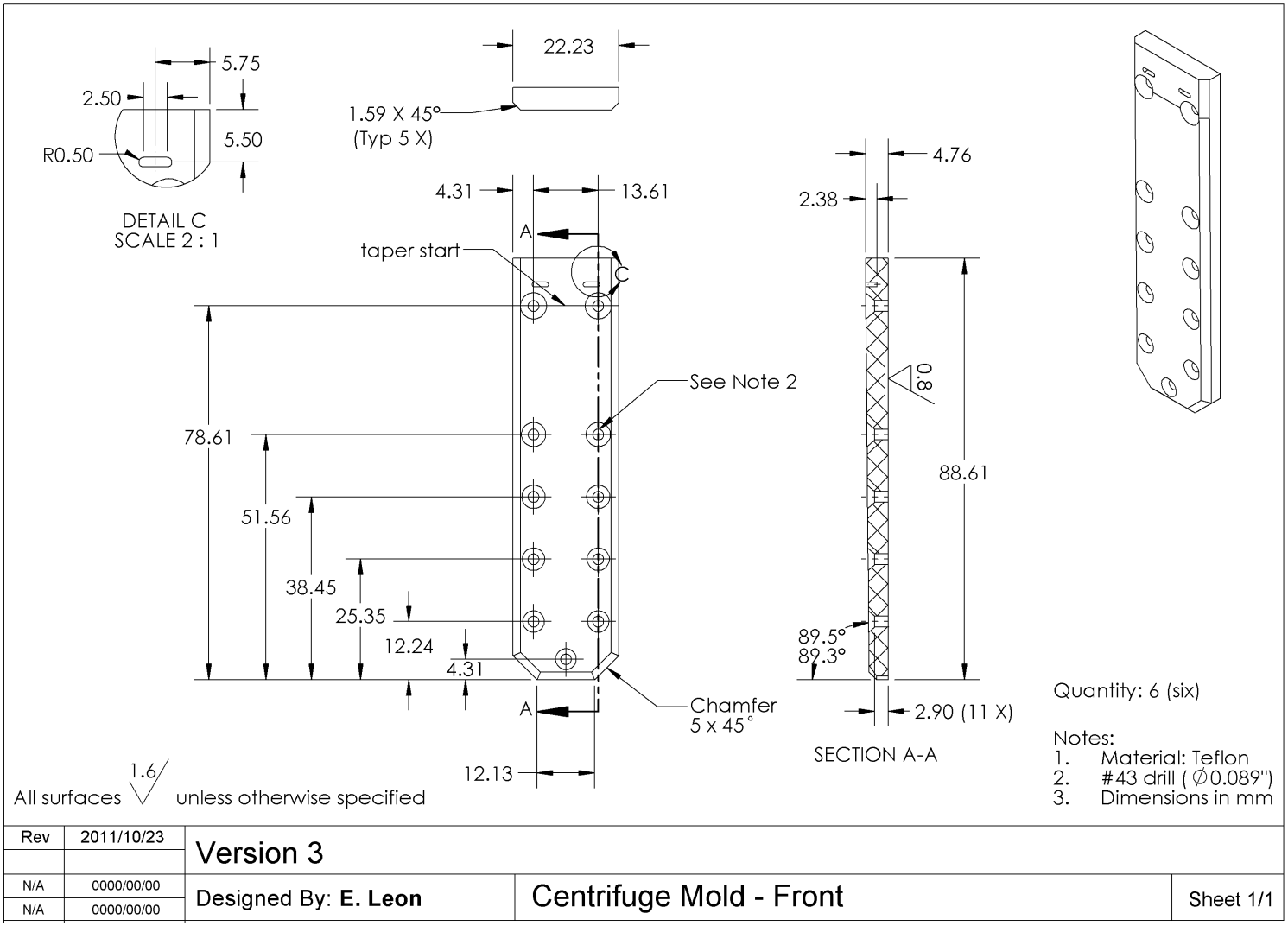

Figure B.5. Centrifuge Mold Front side.

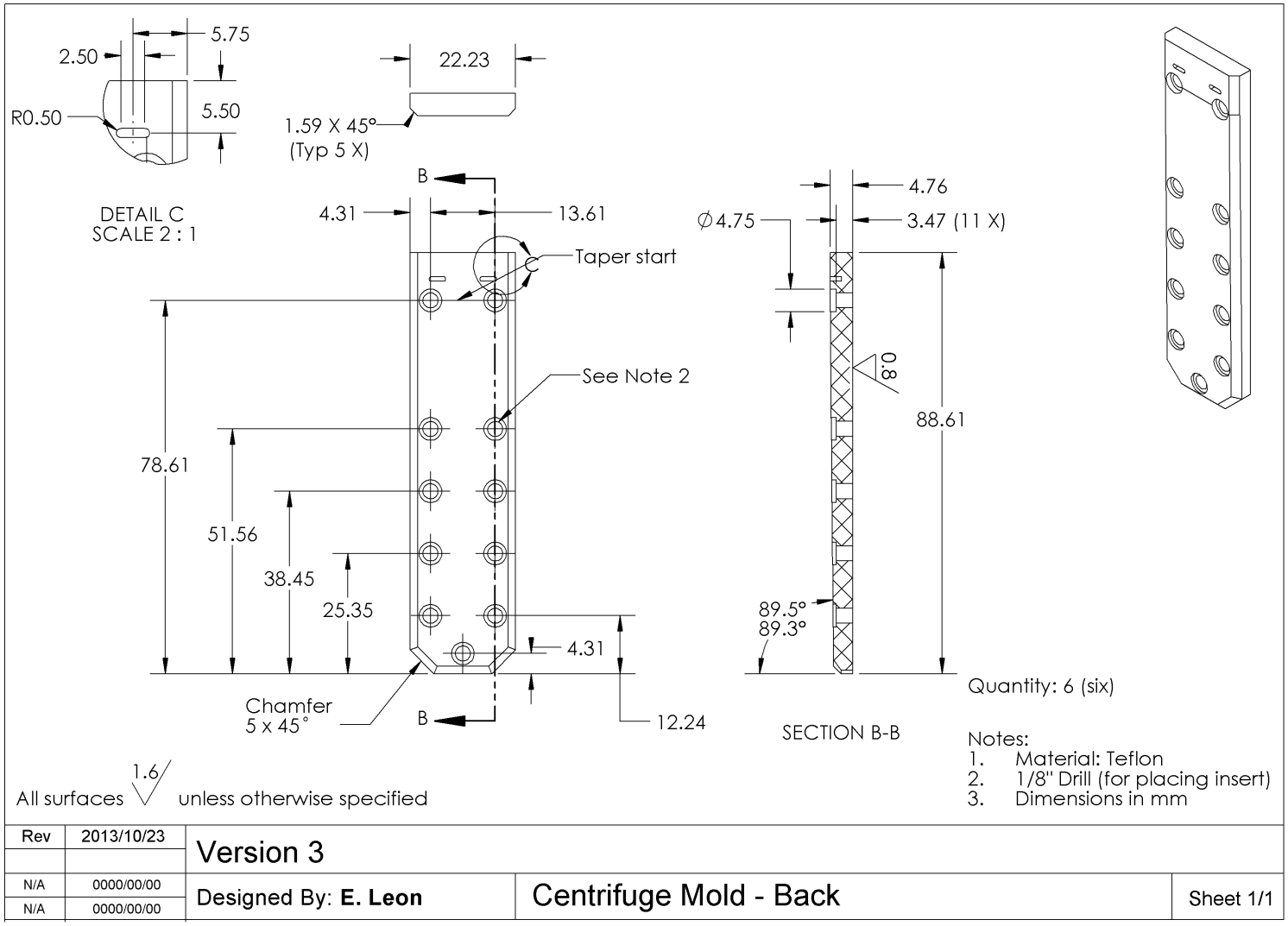

Figure B.6. Centrifuge Mold Back side.

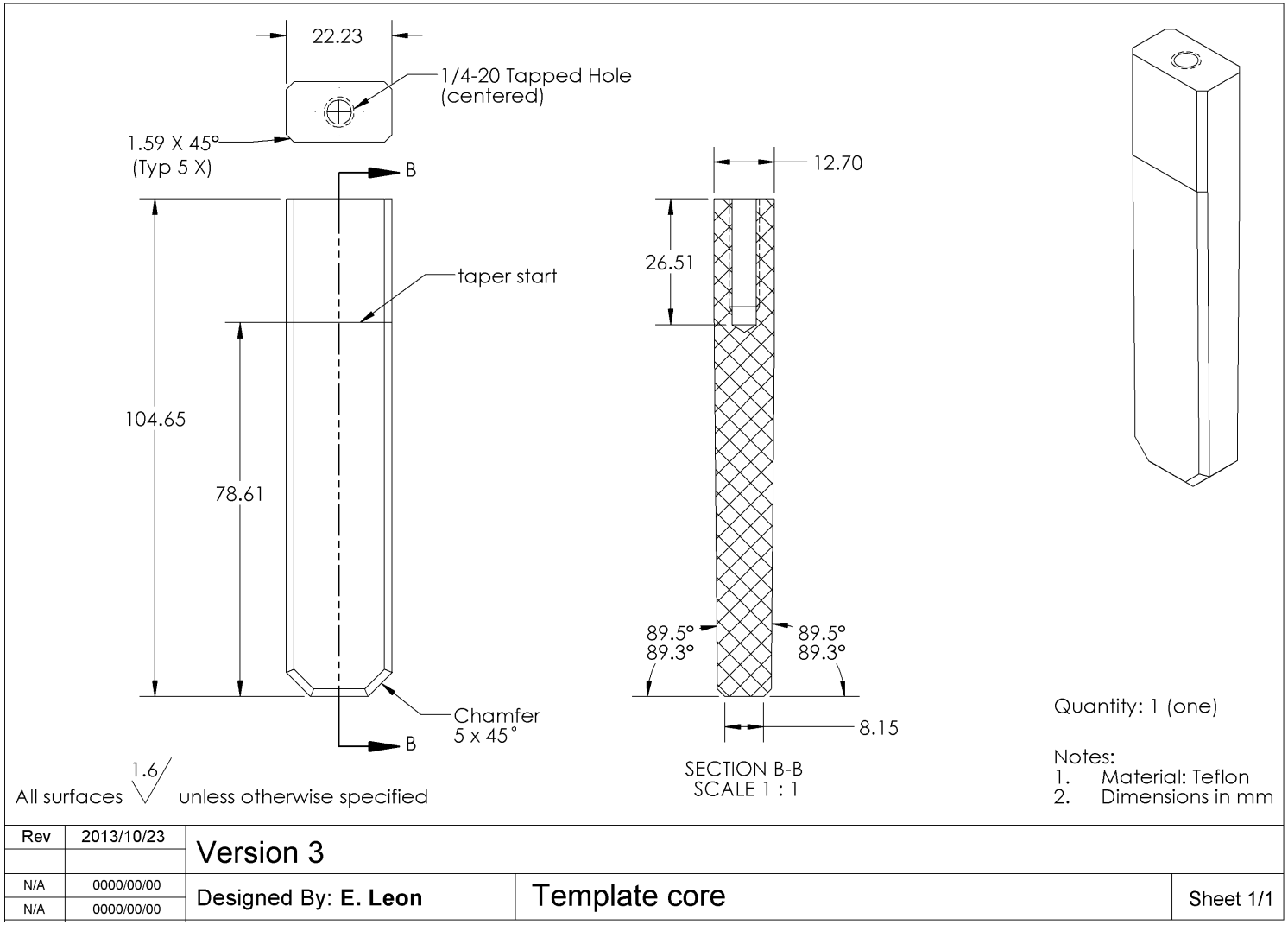

Figure B.7. Template core.

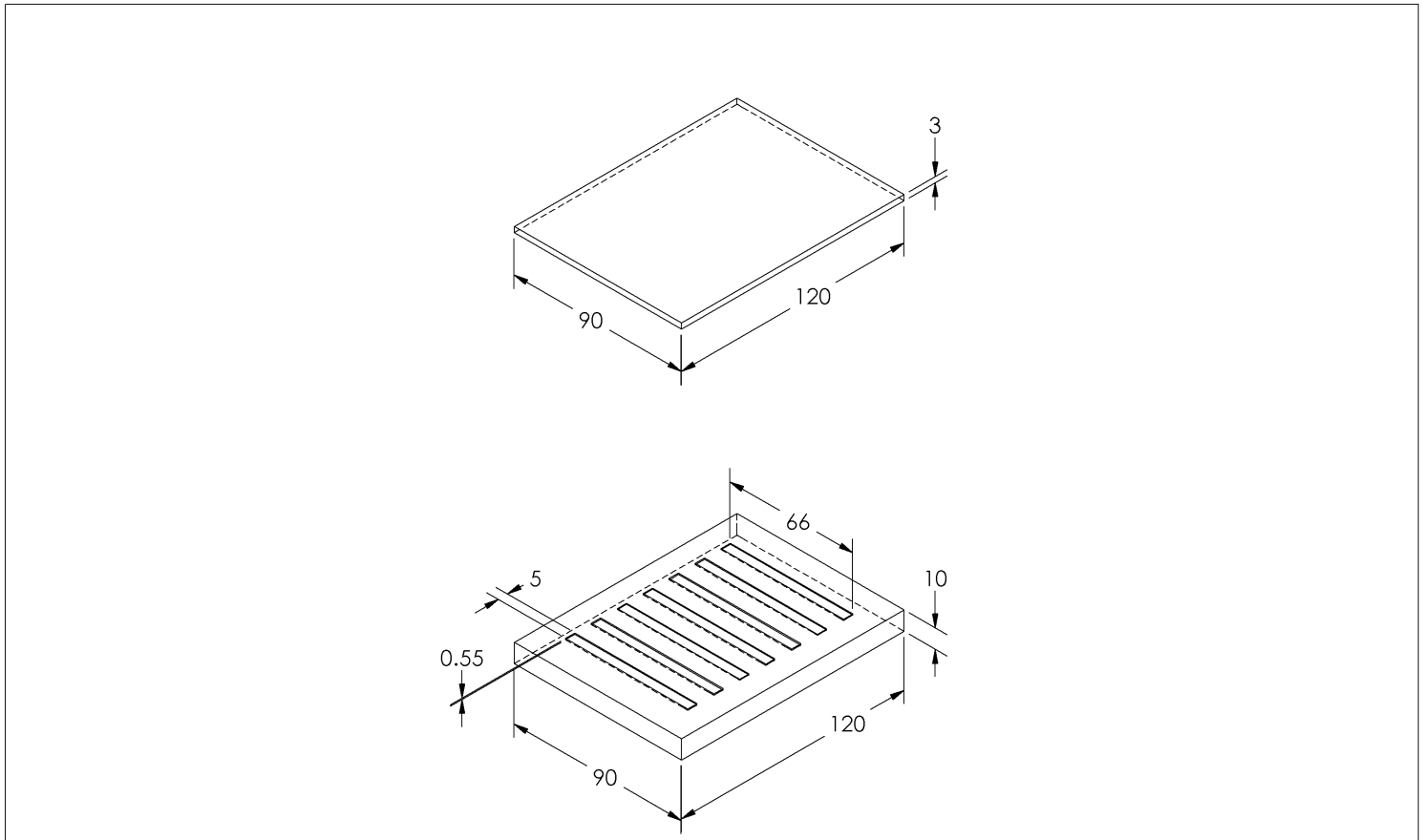

Figure B.8. Silicon mold – Base and Lid.

Appendix C

Analysis of Variance

ANOVA Storage Modulus

As reported by R Studio (v 0.98.1062), the following tables assess the effect of time on the storage modulus for dry and hygrothermal aging conditions and effect of moisture uptake on the storage modulus for the hygrothermal aging conditions.

Effect of Time on Storage Modulus (Dry)

25 °C-0%

```
> anova(SM.sqt.25d)
Analysis of Variance Table

Response: StorageM
          Df Sum Sq Mean Sq F value Pr(>F)
sqrtimeh   1  11225   11225  0.7881  0.378
Residuals 63 897234   14242
```

35 °C-0%

```
> anova(SM.sqt.35d)
Analysis of Variance Table

Response: StorageM
          Df  Sum Sq Mean Sq F value    Pr(>F)
sqrtimeh   1  367379  367379  22.644 1.179e-05 ***
Residuals 63 1022111   16224
---
Signif. codes:  0 ‘***’ 0.001 ‘**’ 0.01 ‘*’ 0.05 ‘.’ 0.1 ‘ ’ 1
```

50 °C-0%

```
> anova(SM.sqt.50d)
Analysis of Variance Table

Response: StorageM
          Df Sum Sq Mean Sq F value    Pr(>F)
sqrtimeh   1 792971  792971   77.01 2.061e-12 ***
Residuals 61 628117   10297
---
Signif. codes:  0 ‘***’ 0.001 ‘**’ 0.01 ‘*’ 0.05 ‘.’ 0.1 ‘ ’ 1
```

Effect of Time on Storage Modulus (Hygrothermal)

35 °C-50%

```
> anova(SM.sqt.3550)
Analysis of Variance Table

Response: StorageM
          Df Sum Sq Mean Sq F value  Pr(>F)
sqr_timeh  1  50869   50869  6.2746 0.01602 *
Residuals 44 356709    8107
---
Signif. codes:  0 ‘***’ 0.001 ‘**’ 0.01 ‘*’ 0.05 ‘.’ 0.1 ‘ ’ 1
```

35 °C-93%

```
> anova(SM.sqt.3593)
Analysis of Variance Table

Response: StorageM
          Df Sum Sq Mean Sq F value Pr(>F)
sqr_timeh  1   4208  4207.9  0.8492 0.3617
Residuals 45 222969  4954.9
```

50 °C-50%

```
> anova(SM.sqt.5050)
Analysis of Variance Table

Response: StorageM
          Df Sum Sq Mean Sq F value Pr(>F)
sqr_timeh  1     17    17.0  0.0026 0.9594
Residuals 44 284866  6474.2
```

50 °C-93%

```
> anova(SM.sqt.5093)
Analysis of Variance Table

Response: StorageM
          Df Sum Sq Mean Sq F value Pr(>F)
sqr_timeh  1   1370  1369.7  0.2616 0.6116
Residuals 44 230373  5235.7
```

25 °C-imm

```
> anova(SM.sqt.25imm)
Analysis of Variance Table

Response: StorageM
          Df Sum Sq Mean Sq F value   Pr(>F)
sqr_timeh  1 203700  203700  10.721 0.002303 **
Residuals 37 703007   19000
---
Signif. codes:  0 ‘***’ 0.001 ‘**’ 0.01 ‘*’ 0.05 ‘.’ 0.1 ‘ ’ 1
```

Effect of Moisture Uptake on Storage Modulus (Hygrothermal)

35 °C-50%

```
> anova(SM.mp.3550)
Analysis of Variance Table

Response: StorageM
          Df Sum Sq Mean Sq F value Pr(>F)
mp         1  35426   35426  4.1884 0.0467 *
Residuals 44 372152    8458
---
Signif. codes:  0 ‘***’ 0.001 ‘**’ 0.01 ‘*’ 0.05 ‘.’ 0.1 ‘ ’ 1
```

35 °C-93%

```
> anova(SM.mp.3593)
Analysis of Variance Table

Response: StorageM
          Df Sum Sq Mean Sq F value  Pr(>F)
mp         1  15694 15693.6  3.3393 0.07428 .
Residuals 45 211484  4699.6
---
Signif. codes:  0 ‘***’ 0.001 ‘**’ 0.01 ‘*’ 0.05 ‘.’ 0.1 ‘ ’ 1
```

50 °C-50%

```
> anova(SM.mp.5050)
Analysis of Variance Table

Response: StorageM
          Df Sum Sq Mean Sq F value  Pr(>F)
mp         1  22430 22430.2  3.7604 0.05891 .
Residuals 44 262453  5964.8
---
Signif. codes:  0 ‘***’ 0.001 ‘**’ 0.01 ‘*’ 0.05 ‘.’ 0.1 ‘ ’ 1
```

50 °C-93%

```
> anova(SM.mp.5093)
Analysis of Variance Table

Response: StorageM
          Df Sum Sq Mean Sq F value    Pr(>F)
mp         1  57106   57106  14.388 0.0004502 ***
Residuals 44 174636    3969
---
Signif. codes:  0 ‘***’ 0.001 ‘**’ 0.01 ‘*’ 0.05 ‘.’ 0.1 ‘ ’ 1
```

25 °C-imm

```
> anova(SM.mp.25imm)
Analysis of Variance Table

Response: StorageM
          Df Sum Sq Mean Sq F value Pr(>F)
mp         1  63889   63889  2.8047 0.1024
Residuals 37 842818   22779
```

ANOVA Maximum Moisture Uptake Study

The following is the ANOVA study for assessing the effects of humidity and temperature on the mass uptake at equilibrium level. The data introduced in R Studio (v 0.98.1062) was categorized by humidity, since visually its significance is evident. The immersed samples were not part of this analysis. Each condition contained three to four replicates and the equilibrium point introduced per replicate was obtained from the average of the four last points at days 58 d, 65 d, 74 d and 80 d (approximately 1396 h, 1562 h, 1778 h and 1923 h) to ensure a correct trend. The sets are presented in Table C.1 and Table C.2.

Table C.1. Mass uptake input data 50%.

Temperature (°C)	Humidity %	Mass Uptake (%)
35	50	1.298
35	50	1.295
35	50	1.375
50	50	1.365
50	50	1.316
50	50	1.181

The null hypothesis (H_0) states that there is no significant difference in yield between the means of mass uptake due to temperature. For the first case in which humidity is set at the lowest level (50%), by comparing conditions 35°C-50% and 50°C-50% it can be inferred by the p-value that temperature has no significant effect in determining the mass uptake at the equilibrium point.

Table C.2. Mass uptake input data 93%.

Temperature (°C)	Humidity %	Mass Uptake (%)
35	93	3.078
35	93	3.137
35	93	2.788
35	93	2.669
50	93	3.156
50	93	3.209
50	93	3.471

```
> summary(cc.50)
            Df  Sum Sq  Mean Sq F value Pr(>F)
temperature  1 0.00188 0.001880   0.338  0.592
Residuals    4 0.02225 0.005563
```

For the second case with humidity at the highest level (93%), by comparing conditions 35°C-93% and 50°C-93%, the resultant p-value of the data collected is shown to be larger but close to 0.05. This suggests that temperature might play a role in establishing the mass uptake at the equilibrium level; however, there is no definite conclusion since the evidence is weak. It is noticeable the apparent trend in the p-values observed between the highest and lowest humidity level, in which a higher humidity generated a smaller p-value (increasing its significance).

```
> summary(cc.93)
            Df Sum Sq Mean Sq F value Pr(>F)
temperature  1 0.2234 0.22337   5.329  0.069 .
Residuals    5 0.2096 0.04192
---
Signif. codes:  0 ‘***’ 0.001 ‘**’ 0.01 ‘*’ 0.05 ‘.’ 0.1 ‘ ’ 1
```

ANOVA T_g Study

The following is the ANOVA table for the T_g and Peaks to diagnose the significance of each parameter, as determined by R Studio (v 0.98.1062). The immersed samples have not been considered in this analysis, to discard possible effects that the different hydrogen bondings might have. There are two null hypotheses where:

H_{01}: There is no significant difference in T_g yield due to temperature.

H_{02}: There is no significant difference in T_g yield due to humidity.

Table C.3. ANOVA input data.

Temperature (°C)	Humidity (%)	Tg E'' (°C)	Tg tan δ (°C)	E'' peak (MPa)	tan δ peak (-)
25	0	131.5	139.6	200.6	0.6961
25	0	129.4	136.8	232.6	0.7395
25	0	129.3	136.6	237.8	0.7423
35	0	128.2	136.1	227.8	0.7173
35	0	130.3	137.8	227.5	0.7256
35	0	127.5	134.8	237.6	0.7464
50	0	131.5	138.6	233.9	0.7323
50	0	129.6	136.7	237.6	0.7456
50	0	128.1	135.7	241.1	0.7457
35	50	126.6	136.7	229.9	0.6946
35	50	130.2	140.8	212.4	0.6667
35	50	128.9	139.6	216.4	0.6648
35	93	112.8	134.5	180.2	0.5169
35	93	112.8	137.1	166.8	0.4682
35	93	113.6	135.9	172.8	0.4838
50	50	127.6	139.3	216.1	0.6726
50	50	129.6	140.5	201	0.6741
50	50	131.4	142.3	168	0.6407
50	93	114.1	140.3	159.7	0.5286
50	93	113.9	141.7	152.2	0.5124
50	93	113.1	139.1	164.2	0.5105

T_g E" (no immersion)

```
> summary(sloss)
                    Df Sum Sq Mean Sq F value   Pr(>F)    
Temperature          1   26.5    26.5   1.470    0.242    
Humidity             1  787.6   787.6  43.649 4.45e-06 ***
Temperature:Humidity 1    0.6     0.6   0.032    0.861    
Residuals           17  306.8    18.0                     
---
Signif. codes:  0 ‘***’ 0.001 ‘**’ 0.01 ‘*’ 0.05 ‘.’ 0.1 ‘ ’ 1
```

T_g *tan* δ (no immersion)

```
> summary(stan)
                     Df Sum Sq Mean Sq F value Pr(>F)
Temperature           1  18.10  18.100   5.087 0.0376 *
Humidity              1   3.04   3.044   0.856 0.3679
Temperature:Humidity  1  21.45  21.445   6.028 0.0252 *
Residuals            17  60.48   3.558
---
Signif. codes:  0 ‘***’ 0.001 ‘**’ 0.01 ‘*’ 0.05 ‘.’ 0.1 ‘ ’ 1
```

Max loss peak (no immersion)

```
> summary(sML)
                     Df Sum Sq Mean Sq F value   Pr(>F)
Temperature           1   1575    1575   7.997   0.0116 *
Humidity              1  13028   13028  66.134 2.92e-07 ***
Temperature:Humidity  1   1117    1117   5.669   0.0292 *
Residuals            17   3349     197
---
Signif. codes:  0 ‘***’ 0.001 ‘**’ 0.01 ‘*’ 0.05 ‘.’ 0.1 ‘ ’ 1
```

Max *tan* δ (no immersion)

```
> summary(sMtan)
                     Df  Sum Sq Mean Sq F value   Pr(>F)
Temperature           1 0.00667 0.00667   5.738   0.0284 *
Humidity              1 0.17198 0.17198 147.935 8.19e-10 ***
Temperature:Humidity  1 0.00000 0.00000   0.004   0.9493
Residuals            17 0.01976 0.00116
---
Signif. codes:  0 ‘***’ 0.001 ‘**’ 0.01 ‘*’ 0.05 ‘.’ 0.1 ‘ ’ 1
```